

Di Stefano, S., Ramírez-Torres, A., Penta, R. and Grillo, A. (2018) Self-influenced growth through evolving material inhomogeneities. *International Journal of Non-Linear Mechanics*, 106, pp. 174-187. (doi: [10.1016/j.ijnonlinmec.2018.08.003](https://doi.org/10.1016/j.ijnonlinmec.2018.08.003))

The material cannot be used for any other purpose without further permission of the publisher and is for private use only.

There may be differences between this version and the published version. You are advised to consult the publisher's version if you wish to cite from it.

<http://eprints.gla.ac.uk/213051/>

Deposited on 06 April 2020

Enlighten – Research publications by members of the University of
Glasgow

<http://eprints.gla.ac.uk>

Self-influenced growth through evolving material inhomogeneities

Salvatore Di Stefano^a, Ariel Ramírez-Torres^a,
Raimondo Penta^b, Alfio Grillo^{a,*}

^a*Dipartimento di Scienze Matematiche (DISMA) “G.L. Lagrange”,
Politecnico di Torino, Corso Duca degli Abruzzi 24, 10129, Torino, Italy
E-mail: {salvatore.distefano ariel.ramirez alfio.grillo}@polito.it*

^b*School of Mathematics and Statistics, Mathematics and Statistics Building,
University of Glasgow, University Place, Glasgow G12 8QQ, UK
E-mail: Raimondo.Penta@glasgow.ac.uk*

Abstract

We reformulate a model of avascular tumour growth in which the tumour tissue is studied as a biphasic medium featuring an interstitial fluid and a solid phase. The description of growth relies on two fundamental features: One of those is given by the mass transfer among the constituents of the phases, which is taken into account through source and sink terms; the other one is the multiplicative decomposition of the deformation gradient tensor of the solid phase, with the introduction of a *growth tensor*, which represents the growth-induced structural changes of the tumour. In general, such tensor is non-integrable, and it may allow to define a Levi-Civita connection with non-trivial curvature. Moreover, its evolution is related to the source and sink of mass of the solid phase through an evolution equation. Our goal is to study how growth can be influenced by the inhomogeneity of the growth tensor. To this end, we study the evolution of the latter, as predicted by two different models. In the first one, the dependence of the growth tensor on the tumour’s material points is not explicitly considered in the evolution equation. In the second model, instead, the inhomogeneity of the growth tensor is resolved explicitly by introducing the curvature associated with it into the evolution equation. Through numerical simulations, we compare the results produced by these two models, and we evaluate a possible role of the material inhomogeneities on growth.

Keywords: Growth, Remodelling, Material inhomogeneities, Inelastic distortions

2010 MSC: 74Bxx, 74Cxx, 74Fxx, 76Sxx, 76Zxx, 92Bxx

*Submitted to the Special Issue “Constitutive Modelling in Biomechanics”

*Corresponding author

Email address: alfio.grillo@polito.it (Alfio Grillo)

15 1. Introduction

16 Because of its repercussion on public health, the study of tumour growth is
 17 a very active research field, to which mathematical modelling can give an im-
 18 portant contribution [1, 2, 3]. A rather standard approach is to answer specific
 19 questions at each scale of interest by formulating dedicated models. These can
 20 be based on Statistical Mechanics [4], Kinetic Theories [5, 6, 7, 8, 9], and Con-
 21 tinuum Mechanics [10, 11] (and references therein), depending on whether
 22 the given problem involves the molecular, cellular, or the tissue scale. One of
 23 the main challenges, however, is to understand the complexes of phenomena
 24 that contribute to initiate the sprouting of a tumour, and to bridge across
 25 the physical scales at which they occur. The difficulty arises, for instance,
 26 when different types of models, conceived for different scales and disciplines,
 27 have to be combined efficiently, and solved simultaneously.

28 Within the framework of Continuum Mechanics, the search for the multi-
 29 scale and interdisciplinary approach outlined above is put into action by
 30 formulating multiphasic models of tumour growth (see e.g. [12, 13, 14, 15,
 31 16, 17]). In such models, growth is described as the mass variation of the solid
 32 phase of the tumour at the expenses of its fluid constituents, and the mass
 33 variation is often viewed as the result of the cooperation of both chemical ad
 34 mechanical factors [18].

35 From the point of view of Mechanics, a relevant aspect of growth is the
 36 occurrence of structural transformations that accompany the “*visible*” mo-
 37 tion of a tissue [19, 20], as well as its gain or loss of mass. All through the
 38 years, a huge amount of literature has been produced on this subject, and
 39 on the related issue of the residual stresses and strains that are expected to
 40 exist in a grown material [21]. In fact, apart from [22] and some other recent
 41 papers (see e.g. [23]), many works usually address the structural evolution of
 42 a medium that grows or remodels by having recourse to the Bilby-Kröner-
 43 Lee decomposition (BKL-decomposition) of the deformation gradient tensor
 44 (see e.g. [10, 15, 19, 24, 25, 26, 27, 28, 29, 30, 31, 32, 33, 34, 35] and the
 45 references therein). For a historically reliable review on the roots of the BKL
 46 decomposition and on its significance in Differential Geometry, the Reader
 47 is referred to [36] (Chapter 1, pp. 10–27) and to [37]. In both cases, the
 48 Authors give due credit to the “old”, yet always up-to-date, ideas that have
 49 led to what we nowadays known as BKL decomposition. In particular, the
 50 review provided in [37] makes the uncommon effort of drawing the attention
 51 of the Reader on some literature that, in spite of its importance, has not
 52 become as popular as it deserved.

53 In the case of growth, the simplest version of the BKL-decomposition
 54 consists of splitting the deformation gradient tensor of a tissue into an ac-

commodating factor and a growth factor (cf. Sect. 2). The latter one, denoted by \mathbf{F}_γ in the following, is often referred to as *growth tensor*, and is taken as the representative of the changes of the tissue’s internal structure.

The main properties of \mathbf{F}_γ are that it is non-integrable in general, and that it may induce a non-Euclidean metric tensor, $\mathbf{C}_\gamma = \mathbf{F}_\gamma^T \cdot \mathbf{F}_\gamma$. The latter can be employed to construct a Levi-Civita connection with a non vanishing fourth-order curvature tensor, \mathbf{R} . This result is consistent with the analysis of Kröner [38], according to whom the stress-free body pieces can be glued together in a non-Euclidean space. We emphasise that, in the context of growth, the concept of curvature has been explored e.g. in [39, 40, 41, 42, 43, 44, 45] (see also [46]).

The introduction of the growth tensor, \mathbf{F}_γ , produces many similarities among growth, finite strain elastoplasticity, and the theory of defects in solids (see e.g. [47, 36] for a review) and, in fact, many biological aspects of growth can be re-interpreted in terms of the evolution of inelastic distortions. One similarity with elastoplasticity is the definition of a stress-free “intermediate configuration”, which exemplifies the conceptual separation between growth and deformation. Actually, the “intermediate configuration” is a collection of tissue pieces rather than a true configuration, and is obtained in two steps: First, by removing all the loads acting on the current configuration of the tissue, and then, by ideally chopping the tissue in small, stress-free pieces [36]. These can be assembled in a reference configuration by means of a transformation that is identifiable with \mathbf{F}_γ^{-1} . Hence, growth can be understood as the reverse process, which maps the tissue pieces from the reference configuration into the intermediate one.

Tensor \mathbf{F}_γ^{-1} is *formally* related to the existence of growth-induced inhomogeneities, [28, 42, 48, 49]. Note that we have emphasised the adverb “formally” because, in our theory, we are not using the concept of “*archetype*” [42, 48, 49]. This notion, instead, is used to define an inhomogeneous body as a body for which it is possible to define a non-singular tensor field, whose inverse is non-integrable [28, 42].

Clearly, the way in which the inhomogeneities evolve depends on the biological problem under study and, thus, on the proposed model of growth. For instance, in [28], a prototypal evolution law for the growth inhomogeneities is set in the form of a relation between Eshelby stress and the rate at which the inhomogeneities themselves are produced. In this case, the law is obtained by following a reduction procedure that requires its compliance with the body’s material symmetries, and with the principles of uniformity, objectivity, and independence of the reference configuration.

A different perspective is considered e.g. in [29, 50], where some phenomenological growth laws are discussed within a chemo-mechanical frame-

work. For arteries [51], an evolution law for the growth tensor is obtained in terms of a generalised Onsager’s relation, in which the driving force of growth is identified with the difference between a suitable measure of mechanical stress and a target stress, referred to as “*homeostatic stress*”.

As long as tumour growth is concerned, the hypothesis is often made that the growth tensor is a pure dilatation [52, 53], thereby depending on one parameter only, denoted by γ and referred to as “growth parameter” in the sequel. In such cases, one has to supply an evolution law for γ (see e.g. (11b) below), which translates the mass balance law for the tissue’s solid phase into a kinematic constraint on γ itself [54, 55, 56, 57]. When this line of thought is followed, the evolution of the growth tensor is entirely dictated by the law describing the variation of mass of the tissue, denoted by r_s in our notation.

Since r_s is related to the rate of change of γ , the problem arises to determine a generalised force that is conjugate to the variation of γ and that, thus, triggers growth. However, since r_s is almost always assigned on the basis of biological observations (see e.g. [55, 56]), which may be phenomenological or “*micro-mechanically motivated*” [10], it may not be possible to identify mechanical stress with the “driving force” that moves the growth-related distortions (i.e., the inhomogeneities, in the jargon of [28, 42]). This is, in fact, a relevant difference with elastoplasticity, in general, and with the models put forward in [28, 51], in which stress plays a central role. Indeed, it should be emphasised that the growth of a tumour may occur also in the absence of stress, whereas it strongly depends on the presence of nutrients, and may result in a loss of mass when these are unavailable. Still, stress may contribute to modulate the way in which the mass change takes place [54, 58]. Perhaps, we might say that, whereas stress is the “starring character” of pure remodelling (be it growth-induced or not), as it can be the trigger of the changes of the tissue’s structure, it is somehow “downgraded” to a modulating factor in the case of pure growth¹.

A rather different approach is suggested in [42], where the concept of “*self-driven*” inhomogeneities is introduced. The underlying idea, framed within the theory of defects in solids, could be rephrased as follows. Assume to have an inhomogeneous solid medium with a non-uniform distribution of defects, which can be modelled as incompatible distortions, and thus associated with \mathbf{F}_γ . Assume, in addition, that the defects interact with each other, and that the strength of their mutual interaction is accounted for by the variability of \mathbf{F}_γ (i.e., the more \mathbf{F}_γ varies, the stronger the interaction is). Then, to adhere to Epstein’s statement [42]:

¹We warmly thank Prof. Luigi Preziosi for several discussions on this issue.

134 “The evolution is intrinsic or self-driven if [...] the inhomogeneity
 135 moves just by virtue of its being there, perhaps in its effort to relax
 136 itself”

137 we claim that the spatial variability of \mathbf{F}_γ is sufficient to initiate a sponta-
 138 neous evolution of \mathbf{F}_γ in time.

139 In our work, we formulate a model of tumour growth based on the the-
 140 ory presented in [42, 54]. We are interested in quantifying how, and to what
 141 extent, the inhomogeneities produced by growth influence the spatiotempo-
 142 ral evolution of γ . For this purpose, we propose a model that merges the
 143 quasi-phenomenological definition of r_s supplied in [54] with the concept of
 144 “self-driven” distortions put forward in [42]. The underlying idea is that the
 145 functional form of the source/sink of mass r_s should be modified by intro-
 146 ducing a term that takes explicitly into account the scalar curvature, κ_γ ,
 147 associated with \mathcal{R} (see Sect. 2.2). Our motivation for undertaking this task,
 148 inspired by [42], is to give a possible answer to the following question:

149 Let us “prepare” the tissue in some grown configuration, with
 150 initial distribution of γ , γ_{in} , corresponding to nonzero curvature,
 151 $\kappa_{\gamma_{\text{in}}}$. Then, giving for granted that growth produces inhomoge-
 152 neities [28, 42], what is the impact of the initial inhomogeneities
 153 on the growth of the tissue in the subsequent instants of time?

154 The remainder of this manuscript is structured as follows: In Sect. 2, we
 155 provide the notation and the fundamental definitions used in our work. In
 156 Sect. 3, we formulate in detail our model of tumour growth. In Sect. 4,
 157 we solve a benchmark problem. In Sect. 5, we comment the results of our
 158 numerical simulations and, finally, in Sect. 6, we summarise our results, and
 159 outline some future research goals.

160 2. Theoretical background

161 2.1. Kinematics of growth

162 We indicate by \mathcal{B} a bounded region of the three-dimensional Euclidean
 163 space, \mathcal{S} , chosen as reference placement for the considered tissue. For every
 164 $X \in \mathcal{B}$ and every $x \in \mathcal{S}$, we introduce the tangent spaces $T_X \mathcal{B}$ and $T_x \mathcal{S}$ and
 165 the tangent bundles $T\mathcal{B} = \sqcup_{X \in \mathcal{B}} T_X \mathcal{B}$ and $T\mathcal{S} = \sqcup_{x \in \mathcal{S}} T_x \mathcal{S}$. Moreover, we
 166 denote by $\mathcal{B}(t) \equiv \chi(\mathcal{B}, t)$ the placement of the tissue at time $t \in \mathcal{I}$, where
 167 $\chi(\cdot, t) : \mathcal{B} \rightarrow \mathcal{S}$ is the *motion* and $\mathcal{I} \subset \mathbb{R}$ an interval of time. The tangent
 168 map $\mathbf{F}(\cdot, t) \equiv T\chi(\cdot, t)$ is the deformation gradient tensor, and is defined as
 169 $\mathbf{F}(\cdot, t) : T\mathcal{B} \rightarrow T\mathcal{S}$, so that, for every $X \in \mathcal{B}$, $\mathbf{F}(X, t)$ maps vectors of
 170 $T_X \mathcal{B}$ into vectors of $T_{\chi(X, t)} \mathcal{S}$, i.e., $\mathbf{F}(X, t) : T_X \mathcal{B} \rightarrow T_{\chi(X, t)} \mathcal{S}$.

Remark 1. *The “classical” definition of reference placement, or configuration, although widely used in Solid Mechanics, may not apply to biological tissues. To the best of our knowledge, this is particularly true for a medium undergoing appositional growth, i.e., the process in which material particles are either deposited on the growing medium, or depleted from it. In both cases, the “number” of material particles constituting the medium varies with time and, consequently, it is impossible to define a unique reference configuration for the medium, at least in the classical sense [22]. Rather, as reported in [22], “the reference configuration of a material point is defined at the time it is deposited,” which means that, at different times, the medium has to be associated with different reference configurations. In our setting, however, we deal with volumetric growth. This type of growth, in fact, still permits the definition of a fixed reference configuration for a growing medium if, as stated in [28], the addition or depletion of material is assumed to occur “in such a way that material points preserve their identity”. With the aid of this hypothesis, we can assume the existence of a fixed reference configuration for the medium under investigation.*

A major character of our theory is the BKL-decomposition, $\mathbf{F} = \mathbf{F}_e \mathbf{F}_\gamma$. As anticipated in the Introduction, \mathbf{F}_γ describes the inelastic changes of the tissue’s internal structure that are induced by growth, while \mathbf{F}_e is the accommodating part of \mathbf{F} , and is assumed to be elastic. Both \mathbf{F}_e and \mathbf{F}_γ are non-singular, and their determinants, $J_e = \det \mathbf{F}_e$ and $J_\gamma = \det \mathbf{F}_\gamma$, are strictly positive.

For every pair $(X, t) \in \mathcal{B} \times \mathcal{I}$, we prescribe that $\mathbf{F}_\gamma(X, t)$ maps vectors of $T_X \mathcal{B}$ into “relaxed” vectors of another tangent space. Such space is denoted by $T_X \mathcal{N}_t$, and can be identified with the image of $T_X \mathcal{B}$ through $\mathbf{F}_\gamma(X, t)$ [45]. Coherently, we write $\mathbf{F}_\gamma(X, t) : T_X \mathcal{B} \rightarrow T_X \mathcal{N}_t$, and, putting together this result and the definition of $\mathbf{F}(X, t)$, we express the elastic part of $\mathbf{F}(X, t)$ as $\mathbf{F}_e(X, t) : T_X \mathcal{N}_t \rightarrow T_{\chi(X, t)} \mathcal{S}$.

In general, the tissue may find itself in a stressed state both in the current and in the reference configuration. Stresses may have different origin but, in the present context, they are generated either by growth or by the loading history undergone by the tissue. Since in our framework growth is the only process regarded as inelastic, it produces stresses that cannot be eliminated by simply switching off the applied loads. Indeed, even though all such loads were suppressed, the tissue would still occupy a configuration in which the growth-induced stresses are nonzero.

As mentioned in the Introduction, to achieve a state in which every part of the tissue is free of stress, one should virtually disassemble the tissue into a “conglomerate” of completely relaxed pieces [38]. Each of such pieces can be

211 thought of as an arbitrarily small neighbourhood of a point $x \in \mathcal{B}_t$, and, for
 212 infinitesimally small neighbourhoods, the body piece associated with x can
 213 be identified with the tangent space $T_x \mathcal{B}_t$. In this case, the whole relaxation
 214 can be viewed as a linear mapping between tangent spaces. In particular,
 215 since the relaxation is elastic, it is represented by $\mathbf{F}_e^{-1}(x, t) : T_x \mathcal{B}_t \rightarrow T_X \mathcal{N}_t$.
 216 Although, $T_X \mathcal{N}_t$ is attached to the same point $X \in \mathcal{B}$ as $T_X \mathcal{B}$, it depends
 217 on time and, above all, it is associated with a state of the tissue characterised
 218 by an important property: it is free of stress, and is obtained by distorting
 219 the elements of $T_X \mathcal{B}$, or the elements of $T_x \mathcal{B}_t$, in a generally incompatible
 220 way. Hence, neither $\mathbf{F}_\gamma(X, t)$ nor $\mathbf{F}_e^{-1}(x, t)$ can be taken as the tangent maps
 221 of deformations evaluated at $X \in \mathcal{B}$ and $x \in \mathcal{B}_t$, respectively. Since this
 222 reasoning applies for each $X \in \mathcal{B}$, the tangent bundle $T\mathcal{N}_t = \sqcup_{X \in \mathcal{B}} T_X \mathcal{N}_t$
 223 cannot be associated with a configuration in the Euclidean space, and \mathcal{N}_t
 224 cannot be claimed to be a configuration in the classical sense. Rather, it
 225 is the *natural*, or ground, state of the tissue, i.e., the state in which the
 226 tissue is free of stress. Such state encompasses the whole structural evolution
 227 undergone by the tissue, which occurs from the reference configuration in the
 228 form of the distortional tensor map $\mathbf{F}_\gamma(\cdot, t) : T\mathcal{B} \rightarrow T\mathcal{N}_t$. A sketch of the
 229 explanation given so far is given in Fig. 1 (left), where \mathcal{N}_t is represented as
 230 a “conglomerate” of stress-free body pieces [38]. We recall, however, that \mathcal{N}_t
 231 can be assembled in a stress-free Riemannian manifold, endowed with the
 232 curved metric induced by \mathbf{F}_γ (cf. e.g. [38, 39, 45]).

233 We notice that, at this stage, \mathbf{F}_γ is not subjected to any restriction.
 234 Hence, granted the polar decompositions $\mathbf{F}_\gamma(X, t) = \mathbf{R}_\gamma(X, t)\mathbf{U}_\gamma(X, t)$ and
 235 $\mathbf{F}_\gamma(X, t) = \mathbf{V}_\gamma(X, t)\mathbf{R}_\gamma(X, t)$, which hold true for each pair $(X, t) \in \mathcal{B} \times \mathcal{I}$,
 236 $\mathbf{F}_\gamma(X, t)$ is generally obtained by combining one of the inelastic stretches,
 237 $\mathbf{U}_\gamma(X, t) : T_X \mathcal{B} \rightarrow T_X \mathcal{B}$ and $\mathbf{V}_\gamma(X, t) : T_X \mathcal{N}_t \rightarrow T_X \mathcal{N}_t$, with the rotation
 238 tensor $\mathbf{R}_\gamma(X, t) : T_X \mathcal{B} \rightarrow T_X \mathcal{N}_t$.

239 Before going further, we mention that a different formulation of the BKL-
 240 decomposition is presented in [59, 60]. The core of such formulation is the
 241 use of two mappings that define a base and a “target” [60] configuration for
 242 each of the factors of the BKL-decomposition. In summary, one indicates by
 243 \mathbf{F}_a and \mathbf{F}_g the accommodating and the growth part of \mathbf{F} , so that $\mathbf{F} = \mathbf{F}_a \mathbf{F}_g$
 244 holds true, and introduces the differentiable mappings χ_a and χ_g such that
 245 \mathbf{F}_a and \mathbf{F}_g are expressed as $\mathbf{F}_a = (T\chi_a)\mathbf{H}_a$ and $\mathbf{F}_g = (T\chi_g)\mathbf{H}_g$ [60]. Here,
 246 $T\chi_a$ and $T\chi_g$ are the tangent maps of χ_a and χ_g , and they represent the
 247 *compatible* contributions to \mathbf{F}_a and \mathbf{F}_g . On the contrary, in general \mathbf{H}_a and
 248 \mathbf{H}_g cannot be identified with the tangent map of any deformation. Indeed,
 249 \mathbf{H}_g describes the generally *incompatible* structural changes due to growth,
 250 while \mathbf{H}_a models the elastic distortions that may have to be applied to the
 251 grown body pieces to restore a global configuration.

For every $t \in \mathcal{I}$, the map $\chi_g(\cdot, t)$ is identified with the diffeomorphism $\chi_g(\cdot, t) : \mathcal{B} \rightarrow \mathcal{C}_t$, where \mathcal{C}_t is referred to as “*intermediate configuration*”, while $T\chi_g(\cdot, t)$ and $\mathbf{H}_g(\cdot, t)$ are defined in terms of maps between tangent spaces, i.e., $T\chi_g(X, t) : T_X\mathcal{B} \rightarrow T_{\chi_g(X, t)}\mathcal{C}_t$ and $\mathbf{H}_g(X, t) : T_X\mathcal{B} \rightarrow T_X\mathcal{B}$, respectively [60]. Analogous considerations hold for $\chi_a(\cdot, t) : \mathcal{C}_t \rightarrow \mathcal{B}_t$ and for $T\chi_a(\cdot, t)$, and $\mathbf{H}_a(\cdot, t)$ (see [60] for details). A drawing summarising the view of the BKL-decomposition presented in [60] is given in Fig. 1 (right). We notice that \mathbf{H}_g plays the same role as \mathbf{F}_γ in the present context.

We emphasise that, although we do not use here the approach by [60], we find it important to draw attention on it because, through χ_g (or χ_a), it introduces an additional degree of freedom that, along with \mathbf{F}_γ , could be useful for other applications of the BKL-decomposition.

In the following, we investigate some consequences of the generally non-integrable nature of \mathbf{F}_γ on the evolution of growth itself (cf. also [39, 45]).

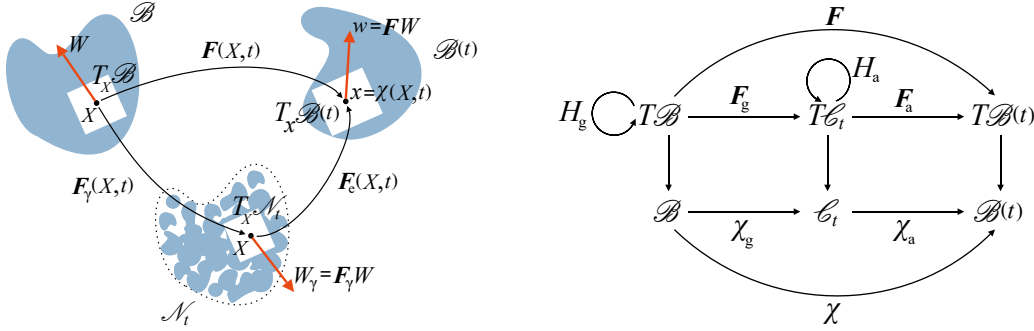


Figure 1: Schematic representation of the introduced mappings.

2.2. Growth and curvature

In this work, \mathbf{F}_γ is assumed to induce the Riemannian metric tensor

$$\mathbf{C}_\gamma = \mathbf{F}_\gamma^T \cdot \mathbf{F}_\gamma, \quad (1)$$

with is said to be the *growth metric tensor*. As pointed out in [59], \mathbf{C}_γ induces a Levi-Civita connection with non-trivial curvature [40, 41]. To see this, we first construct the Christoffel symbols of the connection, which, for a given coordinate system, are given by [61]

$$\Gamma_{MN}^A = \frac{1}{2}(\mathbf{C}_\gamma^{-1})^{AB} \left[\frac{\partial(\mathbf{C}_\gamma)_{BN}}{\partial X^M} + \frac{\partial(\mathbf{C}_\gamma)_{BM}}{\partial X^N} - \frac{\partial(\mathbf{C}_\gamma)_{MN}}{\partial X^B} \right], \quad (2)$$

272 and are symmetric in the lower indices, thereby implying the vanishing of
 273 the torsion [61], i.e.,

$$\mathbf{Tor} = (\Gamma_{MN}^A - \Gamma_{NM}^A) \mathbf{E}_A \otimes \mathbf{E}^M \otimes \mathbf{E}^N = \mathbf{0}. \quad (3)$$

274 Then, we compute the fourth-order curvature tensor generated by \mathbf{C}_γ , i.e.,
 275 $\mathbf{R} = \mathcal{R}_{BMN}^A \mathbf{E}_A \otimes \mathbf{E}^B \otimes \mathbf{E}^M \otimes \mathbf{E}^N$, whose components read [40, 41, 61]

$$\mathcal{R}_{BMN}^A = \frac{\partial \Gamma_{BN}^A}{\partial X^M} - \frac{\partial \Gamma_{BM}^A}{\partial X^N} + \Gamma_{MD}^A \Gamma_{BN}^D - \Gamma_{ND}^A \Gamma_{BM}^D. \quad (4)$$

276 Moreover, by contracting the first and the third index of \mathbf{R} , we obtain the
 277 Ricci curvature tensor,

$$\mathbf{R} = R_{BN} \mathbf{E}^B \otimes \mathbf{E}^N = \mathcal{R}_{BDN}^D \mathbf{E}^B \otimes \mathbf{E}^N, \quad (5)$$

278 and, by double-contracting \mathbf{R} with \mathbf{C}_γ^{-1} , we determine the scalar curvature
 279 associated with growth, i.e.,

$$\kappa_\gamma = \mathbf{R} : \mathbf{C}_\gamma^{-1}. \quad (6)$$

280 3. A model of tumour growth

281 We report on a mathematical model of tumour growth that, in spite of two
 282 important differences, largely follows the path designated in [54]. The first
 283 difference concerns the benchmark problem that we solve, whose geometry is
 284 much simpler than the one used therein. This choice is due to the fact that
 285 we are interested here in purely modelling issues. The second difference, as
 286 anticipated in Sect. 1, concerns the definition of the source/sink term r_s .

287 3.1. Growth and balance laws

288 By adhering to the model of tumour growth developed in [54], we describe
 289 a tumour in avascular stage as a biphasic medium comprising a solid and a
 290 fluid phase. At each point of the tissue, the amount of solid is measured by
 291 means of the apparent mass density $\varphi_s \varrho_s$, where φ_s and ϱ_s are said to be
 292 solid volumetric fraction and true mass density, respectively. Analogously,
 293 the amount of fluid is determined by the apparent density $\varphi_f \varrho_f$, with φ_f
 294 and ϱ_f being the volumetric fraction and true mass density, respectively. We
 295 recall that the *true* mass density of one of the phases constituting a mixture
 296 is the *intrinsic* mass density of the considered phase. In other words, it is
 297 the density that the phase would have if it were present in the mixture with
 298 unitary volumetric fraction. For this reason, the true mass density of a phase
 299 expresses its mass per unit volume of the phase itself, whereas the apparent

300 mass density expresses the phase mass per unit volume of the mixture as a
 301 whole.

302 Within our biphasic model, the tumour represents a saturated porous
 303 medium, so that the condition $\varphi_f = 1 - \varphi_s$ applies. Moreover, the fluid
 304 is assumed to feature only two constituents: a nutrient, with mass fraction
 305 ω_N , and “water”, with mass fraction $\omega_w = 1 - \omega_N$. We hypothesise that ω_N
 306 is very small, so that the mass density of the fluid, ϱ_f , can be regarded as
 307 constant, and approximately equal to the mass density of water. What we
 308 call “water” here is, in fact, a fluid comprising several substances, among
 309 which the constituents of the dead cells that return to the fluid in order to
 310 be expelled.

311 For simplicity, we prescribe that the solid phase consists of two types
 312 of cells only: the proliferating cells, with mass fraction ω_p , and the necrotic
 313 cells, with mass fraction $\omega_n = 1 - \omega_p$. The former ones describe the gain of
 314 mass of the tissue in response to the consumption of the nutrient. However,
 315 they become necrotic when the nutrient falls below a given threshold. The
 316 necrotic cells, in turn, are absorbed by the fluid, thereby accounting for the
 317 tissue’s loss of mass due to cell death. In our model, the transition of a cell
 318 from the proliferating to the necrotic stage preserves the mass density of the
 319 cells. Hence, ϱ_s is independent of the composition of the solid phase, and
 320 may be regarded as constant, in spite of the fact that the mass fractions of
 321 the solid constituents may change in space and time [12, 54, 57].

322 To account for the gain and loss of mass pertaining to the proliferating
 323 and necrotic cells, we introduce their mass balance laws, which we write
 324 under the hypothesis that both types of cells move with the same velocity
 325 \mathbf{v}_s , i.e., the solid phase velocity. By extending the model developed in [54],
 326 we write such balance laws as

$$\partial_t(\varphi_s \varrho_s \omega_p) + \operatorname{div}(\varphi_s \varrho_s \omega_p \mathbf{v}_s) = r_{pn} + r_{fp} + r_{p\gamma}, \quad (7a)$$

$$\partial_t(\varphi_s \varrho_s \omega_n) + \operatorname{div}(\varphi_s \varrho_s \omega_n \mathbf{v}_s) = r_{np} + r_{nf} + r_{n\gamma}, \quad (7b)$$

327 where r_{pn} , r_{fp} , r_{np} , r_{nf} , $r_{p\gamma}$, and $r_{n\gamma}$ denote the rates of mass uptake or
 328 depletion for the solid constituents. In particular, r_{pn} describes the portion
 329 of proliferating cells that, per unit volume and unit time, is converted into
 330 necrotic cells. In turn, r_{np} is the rate at which the necrotic cells are generated
 331 at the expenses of the proliferating ones, so that the condition $r_{pn} + r_{np} = 0$
 332 is respected. Moreover, r_{fp} measures the growth of the proliferating cells
 333 due to the presence of nutrients, while r_{nf} represents the depletion of the
 334 necrotic cells in the fluid. We remark that r_{pn} , r_{fp} , r_{np} , and r_{nf} address
 335 processes that are at the basis of tumour evolution and, in this respect, their
 336 physical interpretation is rather intuitive. On the contrary, $r_{p\gamma}$ and $r_{n\gamma}$ are

introduced to investigate possible consequences of the properties of \mathbf{F}_γ on growth itself. In other words, their task is to establish a feed-back loop among growth, the distortions that it generates, i.e., \mathbf{F}_γ , and the influence of those on the mass exchange terms. To the best of our knowledge, the presence of $r_{p\gamma}$ and $r_{n\gamma}$ in (7a) and (7b) is a novelty in the framework of mathematical modelling of tumour growth.

Since the mass fraction of the necrotic cells can be written as $\omega_n = 1 - \omega_p$, Equation (7b) can be replaced by the mass balance law of the solid phase as a whole. Indeed, by adding together (7a) and (7b), we obtain [54]

$$\partial_t(\varphi_s \varrho_s \omega_p) + \operatorname{div}(\varphi_s \varrho_s \omega_p \mathbf{v}_s) = r_{pn} + r_{fp} + r_{p\gamma}, \quad (8a)$$

$$\partial_t(\varphi_s \varrho_s) + \operatorname{div}(\varphi_s \varrho_s \mathbf{v}_s) = r_s, \quad (8b)$$

where $r_s = r_{fp} + r_{nf} + r_{p\gamma} + r_{n\gamma}$ is the overall source/sink of mass for the solid phase. In general, this term can be diverted into changes either of density or of volume. In this work, since ϱ_s is constant, r_s is diverted into changes of volume. To show this, we perform the backward Piola transformation of (8a) and (8b) by multiplying both equations by $J = \det \mathbf{F}$. Then, by splitting J as $J = J_e J_\gamma$, with $J_e = \det \mathbf{F}_e$ and $J_\gamma = \det \mathbf{F}_\gamma$, we obtain

$$J_\gamma \Phi_{s\nu} \varrho_s \dot{\omega}_p = J[r_{pn} + r_{fp} + r_{p\gamma} - \omega_p r_s], \quad (9a)$$

$$\dot{(J_\gamma \Phi_{s\nu} \varrho_s)} = J r_s = J[r_{fp} + r_{nf} + r_{p\gamma} + r_{n\gamma}], \quad (9b)$$

where $\Phi_{s\nu} := J_e \varphi_s$ is the volumetric fraction of the solid phase expressed per unit volume of the intermediate, stress-free configuration. We require now that $\Phi_{s\nu}$ is constant in time. Since ϱ_s is constant too, the left-hand-side of (9b) is proportional to $\dot{J}_\gamma = J_\gamma \operatorname{tr}[\dot{\mathbf{F}}_\gamma \mathbf{F}_\gamma^{-1}]$. Hence, (9a) and (9b) become

$$\dot{\omega}_p = \frac{J[r_{pn} + r_{fp} + r_{p\gamma} - \omega_p r_s]}{J_\gamma \Phi_{s\nu} \varrho_s}, \quad (10a)$$

$$\operatorname{tr}[\dot{\mathbf{F}}_\gamma \mathbf{F}_\gamma^{-1}] = \frac{J[r_{fp} + r_{nf} + r_{p\gamma} + r_{n\gamma}]}{\Phi_{s\nu} \varrho_s J_\gamma}. \quad (10b)$$

In general, besides varying the mass of a tissue, growth may also induce isochoric distortions. Accordingly, \mathbf{F}_γ can be written as $\mathbf{F}_\gamma = [\det \mathbf{F}_\gamma]^{1/3} \bar{\mathbf{F}}_\gamma$, where $[\det \mathbf{F}_\gamma]^{1/3}$ measures the tissue's volume changes, and $\bar{\mathbf{F}}_\gamma$ is a volume-preserving tensor field that keeps track of the tissue's remodelling at constant mass. Thus, by adopting the notation $\gamma \equiv [\det \mathbf{F}_\gamma]^{1/3}$, we obtain [54]

$$\dot{\omega}_p = \frac{J[r_{pn} + r_{fp} + r_{p\gamma} - \omega_p r_s]}{J_\gamma \Phi_{s\nu} \varrho_s}, \quad (11a)$$

$$\frac{\dot{\gamma}}{\gamma} = \frac{J[r_{\text{fp}} + r_{\text{nf}} + r_{\text{p}\gamma} + r_{\text{n}\gamma}]}{3\Phi_{\text{sv}}\varrho_{\text{s}}J_{\gamma}}. \quad (11\text{b})$$

Remark 2. *The hypothesis of constant true mass density of the solid phase is due to the fact that such phase is considered to be a representation of the tissue's cells. These, in turn, are essentially made of water, whose mass density is constant in the biophysical range relevant to our work. It follows, thus, that also ϱ_{s} can be safely assumed to be constant. However, if this assumption is relaxed, Eq. (8b) can be recast in the form*

$$\overline{\dot{\varphi}_{\text{s}}\varrho_{\text{s}}} + \varphi_{\text{s}}\varrho_{\text{s}}\text{div}\mathbf{v}_{\text{s}} = r_{\text{s}}, \quad (12)$$

and, by exploiting the identity $\dot{J} = J(\text{div}\mathbf{v}_{\text{s}})$, one can write

$$J\dot{\varphi}_{\text{s}}\varrho_{\text{s}} + J\varphi_{\text{s}}\dot{\varrho}_{\text{s}} + \dot{J}\varphi_{\text{s}}\varrho_{\text{s}} = Jr_{\text{s}}. \quad (13)$$

Since it holds that $\dot{J} = \dot{J}_{\text{e}}J_{\text{g}} + J_{\text{e}}\dot{J}_{\gamma} = J\text{tr}[\mathbf{L}_{\text{e}}] + J\text{tr}[\mathbf{L}_{\gamma}]$, with $\mathbf{L}_{\text{e}} = \dot{\mathbf{F}}_{\text{e}}\mathbf{F}_{\text{e}}^{-1}$ and $\mathbf{L}_{\gamma} = \dot{\mathbf{F}}_{\gamma}\mathbf{F}_{\gamma}^{-1}$, one obtains

$$J\dot{\varphi}_{\text{s}}\varrho_{\text{s}} + J\varphi_{\text{s}}\dot{\varrho}_{\text{s}} + J\varphi_{\text{s}}\varrho_{\text{s}}\text{tr}[\mathbf{L}_{\text{e}}] + J\varphi_{\text{s}}\varrho_{\text{s}}\text{tr}[\mathbf{L}_{\gamma}] = Jr_{\text{s}}. \quad (14)$$

Moreover, we require $\text{tr}[\mathbf{L}_{\gamma}] = r_{\text{s}}/(\varphi_{\text{s}}\varrho_{\text{s}})$, so that (14) becomes

$$\dot{\varphi}_{\text{s}}\varrho_{\text{s}} + \varphi_{\text{s}}\dot{\varrho}_{\text{s}} + \varphi_{\text{s}}\varrho_{\text{s}}\text{tr}[\mathbf{L}_{\text{e}}] = 0, \quad (15)$$

which can be equivalently rearranged as $\overline{J_{\text{e}}\dot{\varphi}_{\text{s}}\varrho_{\text{s}}} = 0$. Thus, only the product $\varphi_{\text{s}}\varrho_{\text{s}}$, which individuates the mass density of the solid phase, is constant in time. Without loss of generality, it can be expressed with respect to the natural state, i.e., for $J_{\text{e}} = 1$, as

$$J_{\text{e}}\varphi_{\text{s}}\varrho_{\text{s}} = \Phi_{\text{sv}}\varrho_{\text{s}0}, \quad (16)$$

where Φ_{sv} is the volumetric fraction in the natural state, and $\varrho_{\text{s}0}$ denotes a constant reference value of the solid phase mass density. Equation (16) implies that $\varphi_{\text{s}}\varrho_{\text{s}}$ is a function of the elastic part of the overall deformation gradient tensor through J_{e} . In this case, ϱ_{s} can be either treated as an independent variable of the theory or specified through a state law. If the first option is chosen, the model necessitates an additional equation determining the volumetric fraction (cf. e.g. [62, 63, 64]). If, instead, the second choice is made, and one assumes that ϱ_{s} is a constitutive function e.g. of the com-

383 position of the solid phase, one obtains

$$\varphi_s = \frac{\Phi_{sv}\hat{\varrho}_s(\omega_{p0})}{J_e\hat{\varrho}_s(\omega_p)} = \frac{J_\gamma\Phi_{sv}\hat{\varrho}_s(\omega_{p0})}{J\hat{\varrho}_s(\omega_p)}. \quad (17)$$

384 Here, $\hat{\varrho}_s(\omega_p)$ is the constitutive representation of the true mass density of the
 385 solid phase. As anticipated above, it is specified as a function of the com-
 386 position of the solid phase, which, within our model, is determined by the
 387 amount of proliferant and necrotic cells. Since it holds that $\omega_p + \omega_n = 1$, is
 388 suffices to use only one of the two mass fractions ω_p and ω_n to characterise
 389 the composition. Upon choosing ω_p , we let $\hat{\varrho}_s$ depend on ω_p only, and we take
 390 ω_{p0} as a reference value for ω_p .

391 In conjunction with (11a) and (11b), also the mass balance laws of the
 392 nutrients and the fluid phase as a whole need to be studied

$$\partial_t(\varphi_f\varrho_f\omega_N) + \operatorname{div}(\varphi_f\varrho_f\omega_N\mathbf{v}_f + \mathbf{y}_N) = r_{Np}, \quad (18a)$$

$$\partial_t(\varphi_f\varrho_f) + \operatorname{div}(\varphi_f\varrho_f\mathbf{v}_f) = -r_s. \quad (18b)$$

393 In (18a) and (18b), \mathbf{v}_f is the velocity of the fluid, \mathbf{y}_N is the mass flux vector
 394 associated with the motion of the nutrients relative to the fluid phase, and r_{Np}
 395 is the rate at which the nutrients are “eaten” by the proliferating cells. We
 396 remark that, to ensure the conservation of the mass of the biphasic medium
 397 under study, the right-hand-side of (18b) is taken equal to the negative of r_s .

398 After some calculations, (18a) and (18b) can be rephrased as

$$\varphi_f\varrho_f\dot{\omega}_N + \varrho_f\mathbf{q} \operatorname{grad}\omega_N + \operatorname{div}\mathbf{y}_N = r_{Np} + \omega_N r_s, \quad (19a)$$

$$\operatorname{div}\mathbf{q} + \operatorname{div}\mathbf{v}_s = \left(\frac{1}{\varrho_s} - \frac{1}{\varrho_f}\right) r_s, \quad (19b)$$

399 where $\mathbf{q} = \varphi_f[\mathbf{v}_f - \mathbf{v}_s]$ is said to be filtration velocity. Finally, (19a) and (19b)
 400 can be pulled-back to the reference configuration, thereby obtaining

$$(J - J_g\Phi_{sv})\varrho_f\dot{\omega}_N + \varrho_f\mathbf{Q} \operatorname{Grad}\omega_N + \operatorname{Div}\mathbf{Y}_N = J[r_{Np} + \omega_N r_s], \quad (20a)$$

$$\operatorname{Div}\mathbf{Q} + j = \left(\frac{1}{\varrho_s} - \frac{1}{\varrho_f}\right) J r_s, \quad (20b)$$

401 where $\mathbf{Q} = J\mathbf{F}^{-1}\mathbf{q}$ is the material filtration velocity, and $\mathbf{Y}_N = J\mathbf{F}^{-1}\mathbf{y}_N$
 402 is the material mass flux vector of the nutrients. Under the hypothesis of
 403 validity of Darcy’s law for the fluid, and of Fick’s law for the nutrients, \mathbf{Q} and
 404 \mathbf{Y}_N read $\mathbf{Q} = -\mathbf{K}\operatorname{Grad}p$ and $\mathbf{Y}_N = -\varrho_f\mathbf{D}\operatorname{Grad}\omega_N$, with $\mathbf{K} = J\mathbf{F}^{-1}\mathbf{k}\mathbf{F}^{-T}$
 405 being the material permeability, p the pore pressure, and $\mathbf{D} = J\mathbf{F}^{-1}\mathbf{d}\mathbf{F}^{-T}$

the material diffusivity tensor of the nutrients in water. The tensors \mathbf{K} and \mathbf{D} are the backward Piola transforms of the spatial permeability, \mathbf{k} , and of the spatial diffusivity, \mathbf{d} , respectively.

To conclude, we introduce the momentum balance law for the biphasic medium as a whole, which we write directly in material form (see [54] for details), i.e.,

$$\text{Div} \left(-Jp \mathbf{g}^{-1} \mathbf{F}^{-T} + \mathbf{P}_{\text{sc}} \right) = \mathbf{0}, \quad (21)$$

where \mathbf{P}_{sc} is referred to as the constitutive part of the first Piola-Kirchhoff stress tensor of the solid phase.

3.2. Constitutive laws

In this work, the tumour tissue is assumed to be isotropic, and, for simplicity, \mathbf{k} and \mathbf{d} are taken “*unconditionally isotropic*” [65], which means that they are both proportional to the inverse metric tensor \mathbf{g}^{-1} . Hence, we write $\mathbf{k} = k_0 \mathbf{g}^{-1}$ and $\mathbf{d} = d_0 \mathbf{g}^{-1}$, where k_0 is given in the form of the Holmes-Mow scalar permeability [65, 66], and d_0 is defined as a function of J and J_γ through the fluid phase volumetric fraction, i.e.,

$$\begin{aligned} k_0 &= k_{0\text{R}} \left[\frac{\Phi_{s\nu} \varphi_{\text{f}}}{\varphi_{\text{f}0} \varphi_{\text{s}}} \right]^{m_0} \exp \left(\frac{m_1}{2} \left[\frac{J^2 - J_\gamma^2}{J_\gamma^2} \right] \right) \\ &= k_{0\text{R}} \left[\frac{J - J_\gamma \Phi_{s\nu}}{J_\gamma \varphi_{\text{f}0}} \right]^{m_0} \exp \left(\frac{m_1}{2} \left[\frac{J^2 - J_\gamma^2}{J_\gamma^2} \right] \right), \end{aligned} \quad (22a)$$

$$d_0 = \varphi_{\text{f}} d_{0\text{R}} = \frac{J - J_\gamma \Phi_{s\nu}}{J} d_{0\text{R}}. \quad (22b)$$

In (22a), $\varphi_{\text{f}0} = 1 - \Phi_{s\nu}$ is a reference value of the fluid phase volumetric fraction, m_0 and m_1 are constant material coefficients, and $k_{0\text{R}}$ is said to be the reference permeability of the medium. This quantity is assumed to be a constant in this work, even though it should be defined as a function of material points in a more general setting. The factor $d_{0\text{R}}$ in (22b) is the reference diffusivity, which, for simplicity, is assumed here to be constant. This condition, in fact, may be violated when the nutrient mass fraction, ω_{N} , is sufficiently greater than zero, in which case $d_{0\text{R}}$ should be defined as a function of ω_{N} .

By substituting (22a) and (22b) into the definitions of \mathbf{k} and \mathbf{d} , and the corresponding results into the expressions of the material permeability and diffusivity, we find

$$\mathbf{K} = J k_0 \mathbf{C}^{-1}, \quad (23a)$$

$$\mathbf{D} = (J - J_\gamma \Phi_{s\nu}) d_{0\text{R}} \mathbf{C}^{-1}. \quad (23b)$$

432 Besides being isotropic, the solid phase of the tissue is assumed to be
 433 hyperelastic. Hence, its mechanical behaviour can be described by means of
 434 a strain energy density function, \mathcal{W} , which we express per unit volume of
 435 the reference configuration. To account for the variation of internal structure
 436 induced by growth, \mathcal{W} is given in terms of a constitutive function, $\tilde{\mathcal{W}}$, of \mathbf{F} ,
 437 \mathbf{F}_γ , and material points, X . The purely elastic contribution of the material
 438 to the overall energy can be measured by introducing the energy density \mathcal{W}_ν ,
 439 defined per unit volume of the stress-free configuration, whose associated
 440 constitutive representation, $\tilde{\mathcal{W}}_\nu$, depends on \mathbf{F} and \mathbf{F}_γ exclusively through
 441 \mathbf{F}_e . Hence, we write [28] (see also [67] for details)

$$\mathcal{W} = J_\gamma \mathcal{W}_\nu, \quad \tilde{\mathcal{W}}(\mathbf{F}, \mathbf{F}_\gamma, X) = J_\gamma \tilde{\mathcal{W}}_\nu(\mathbf{F}_e). \quad (24)$$

442 For $\tilde{\mathcal{W}}_\nu(\mathbf{F}_e)$, we choose a constitutive law of the Holmes-Mow type [66], i.e.,

$$\begin{aligned} \tilde{\mathcal{W}}_\nu(\mathbf{F}_e) &= \hat{\mathcal{W}}_\nu(\mathbf{C}_e) = \check{\mathcal{W}}_\nu(\hat{I}_1(\mathbf{C}_e), \hat{I}_2(\mathbf{C}_e), \hat{I}_3(\mathbf{C}_e)) \\ &= \alpha_0 \left\{ \exp(\hat{\Psi}(\mathbf{C}_e)) - 1 \right\}, \end{aligned} \quad (25a)$$

$$\begin{aligned} \hat{\Psi}(\mathbf{C}_e) &= \check{\Psi}(\hat{I}_1(\mathbf{C}_e), \hat{I}_2(\mathbf{C}_e), \hat{I}_3(\mathbf{C}_e)) \\ &= \alpha_1 [\hat{I}_1(\mathbf{C}_e) - 3] + \alpha_2 [\hat{I}_2(\mathbf{C}_e) - 3] - \alpha_3 \ln(\hat{I}_3(\mathbf{C}_e)), \end{aligned} \quad (25b)$$

443 where $\mathbf{C}_e = \mathbf{F}_e^T \cdot \mathbf{F}_e$ is the elastic Cauchy-Green deformation tensor, $\hat{\mathcal{W}}_\nu(\mathbf{C}_e)$
 444 is introduced to comply with objectivity, and, to account for isotropy, the
 445 dependence of $\check{\mathcal{W}}_\nu$ on \mathbf{C}_e is expressed through the principal invariants

$$I_1 = \hat{I}_1(\mathbf{C}_e) = \text{tr}(\boldsymbol{\eta}^{-1} \mathbf{C}_e), \quad (26a)$$

$$I_2 = \hat{I}_2(\mathbf{C}_e) = \frac{1}{2} \{ [\hat{I}_1(\mathbf{C}_e)]^2 - \text{tr}[(\boldsymbol{\eta}^{-1} \mathbf{C}_e)^2] \}, \quad (26b)$$

$$I_3 = \hat{I}_3(\mathbf{C}_e) = \det \mathbf{C}_e. \quad (26c)$$

446 Here, $\boldsymbol{\eta}$ is the metric tensor of the intermediate configuration and, by using
 447 the equality $\mathbf{C}_e = \mathbf{F}_\gamma^{-T} \mathbf{C} \mathbf{F}_\gamma^{-1}$, it can be eliminated from (26a)–(26c), so that
 448 the invariants can be rephrased as functions of \mathbf{C} and \mathbf{C}_γ . Finally, in (25b),
 449 the material coefficients α_0 , α_1 , α_2 , and α_3 are functions of Lamé's elastic
 450 parameters [68] (in particular, as in [66], we set $\alpha_3 = 1$), i.e.,

$$\alpha_0 = \frac{2\mu + \lambda}{4\alpha_3}, \quad \alpha_1 = \alpha_3 \frac{2\mu - \lambda}{2\mu + \lambda}, \quad \alpha_2 = \alpha_3 \frac{\lambda}{2\mu + \lambda}, \quad \alpha_3 = \alpha_1 + 2\alpha_2. \quad (27)$$

451 Equations (24), (25a), (25b), and (26a)–(26c) permit to calculate the consti-

452 tutive part of the second Piola-Kirchhoff stress tensor of the solid phase:

$$\begin{aligned}\mathbf{S}_{\text{sc}} &= \hat{\mathbf{S}}_{\text{sc}}(\mathbf{C}, \mathbf{C}_\gamma) = \left[J_\gamma \mathbf{F}_\gamma^{-1} \left(2 \frac{\partial \hat{\mathcal{W}}_\nu}{\partial \mathbf{C}_e}(\mathbf{C}_e) \right) \mathbf{F}_\gamma^{-\text{T}} \right] \\ &= 2J_\gamma b_1 \mathbf{C}_\gamma^{-1} + 2J_\gamma b_2 [I_1 \mathbf{C}_\gamma^{-1} - \mathbf{C}_\gamma^{-1} \mathbf{C} \mathbf{C}_\gamma^{-1}] + 2J_\gamma b_3 I_3 \mathbf{C}^{-1},\end{aligned}\quad (28)$$

453 with $b_i = \partial \check{W}_\nu / \partial I_i$, $i \in \{1, 2, 3\}$. Consequently, the first Piola-Kirchhoff
454 stress tensor \mathbf{P}_{sc} can be expressed constitutively as

$$\mathbf{P}_{\text{sc}} = \hat{\mathbf{P}}_{\text{sc}}(\mathbf{F}, \mathbf{C}_\gamma) = \mathbf{F} \hat{\mathbf{S}}_{\text{sc}}(\mathbf{C}, \mathbf{C}_\gamma), \quad (29)$$

455 and, thus, the constitutive part of the Cauchy stress tensor reads

$$\begin{aligned}\boldsymbol{\sigma}_{\text{sc}} &= \hat{\boldsymbol{\sigma}}_{\text{sc}}(\mathbf{F}, \mathbf{C}_\gamma) = J^{-1} \hat{\mathbf{P}}_{\text{sc}}(\mathbf{F}, \mathbf{C}_\gamma) \mathbf{F}^{\text{T}} \\ &= \frac{J_\gamma}{J} \{ 2b_1 \mathbf{b}_e + 2b_2 [I_1 \mathbf{b}_e - \mathbf{b}_e \cdot \mathbf{b}_e] + 2b_3 I_3 \mathbf{g}^{-1} \},\end{aligned}\quad (30)$$

456 where $\mathbf{b}_e = \mathbf{F} \mathbf{C}_\gamma^{-1} \mathbf{F}^{\text{T}}$ is the elastic right Cauchy-Green deformation tensor.

457 3.3. Sources and sinks of mass

458 To model growth, it is necessary to describe the mass exchanges among
459 the constituents of the system under study. In our framework, this requires to
460 provide mathematical expressions for r_{fp} , r_{pn} , r_{nf} , and r_{Np} , and to relate each
461 of these quantities with the appropriate set of chemo-mechanical variables.
462 For r_{pn} , r_{nf} , and r_{Np} , we adopt the phenomenological expressions suggested
463 in [54], which we report here with slight changes of notation, i.e.,

$$r_{\text{pn}} = -\zeta_{\text{pn}} \left\langle 1 - \frac{\omega_{\text{N}}}{\omega_{\text{Ncr}}} \right\rangle_+ \varphi_{\text{s}} \omega_{\text{p}} = -\zeta_{\text{pn}} \left\langle 1 - \frac{\omega_{\text{N}}}{\omega_{\text{Ncr}}} \right\rangle_+ \frac{J_\gamma \Phi_{\text{sv}}}{J} \omega_{\text{p}}, \quad (31\text{a})$$

$$r_{\text{nf}} = -\zeta_{\text{nf}} \varphi_{\text{s}} [1 - \omega_{\text{p}}] = -\zeta_{\text{nf}} \frac{J_\gamma \Phi_{\text{sv}}}{J} [1 - \omega_{\text{p}}], \quad (31\text{b})$$

$$r_{\text{Np}} = -\zeta_{\text{Np}} \frac{\omega_{\text{N}}}{\omega_{\text{N}} + \omega_{\text{N0}}} \varphi_{\text{s}} \omega_{\text{p}} = -\zeta_{\text{Np}} \frac{\omega_{\text{N}}}{\omega_{\text{N}} + \omega_{\text{N0}}} \frac{J_\gamma \Phi_{\text{sv}}}{J} \omega_{\text{p}}, \quad (31\text{c})$$

$$\begin{aligned}r_{\text{fp}} &= \zeta_{\text{fp}} \left\langle \frac{\omega_{\text{N}} - \omega_{\text{Ncr}}}{\omega_{\text{Nenv}} - \omega_{\text{Ncr}}} \right\rangle_+ \left[1 - \frac{\delta_1 \langle \bar{\sigma} \rangle_+}{\delta_2 + \langle \bar{\sigma} \rangle_+} \right] \frac{\varphi_{\text{f}} \varphi_{\text{s}}}{\varphi_{\text{f0}}} \omega_{\text{p}} \\ &= \zeta_{\text{fp}} \left\langle \frac{\omega_{\text{N}} - \omega_{\text{Ncr}}}{\omega_{\text{Nenv}} - \omega_{\text{Ncr}}} \right\rangle_+ \left[1 - \frac{\delta_1 \langle \bar{\sigma} \rangle_+}{\delta_2 + \langle \bar{\sigma} \rangle_+} \right] \frac{J - J_\gamma \Phi_{\text{sv}}}{J \varphi_{\text{f0}}} \frac{J_\gamma \Phi_{\text{sv}}}{J} \omega_{\text{p}}.\end{aligned}\quad (31\text{d})$$

464 The terms r_{pn} , r_{nf} , and r_{Np} are sinks of mass for the constituents to which
465 they refer. In particular, r_{pn} represents the loss of mass of the proliferant
466 cells that become necrotic. The term r_{fp} , instead, is a source of mass for

the proliferant cells, and represents the mass gained by this population of cells at the expenses of the fluid. We need to emphasise that both r_{pn} and r_{fp} represent processes whose occurrence is strongly controlled by the availability of the nutrients in the tissue. To describe mathematically the concept of “availability of the nutrients”, we introduce a critical value of the nutrients’ mass fraction, $\omega_{\text{Ncr}} \in]0, 1[$, and we model the transfers of mass associated with r_{pn} and r_{fp} as threshold processes. Accordingly, when it holds that $\omega_{\text{N}} \leq \omega_{\text{Ncr}}$, the proliferant cells die, which means that r_{pn} is active, while r_{fp} is switched off. On the contrary, for $\omega_{\text{N}} > \omega_{\text{Ncr}}$, r_{pn} must vanish identically, whereas r_{fp} is switched on. Such activation and deactivation of r_{pn} and r_{fp} is formulated by means of the operator $\langle \cdot \rangle_+$, which returns the argument to which it is applied, when the argument is greater than zero, and zero otherwise. Thus, it is introduced to switch off cell death when the mass fraction of the nutrients, ω_{N} , is above, or equal to, the threshold level $\omega_{\text{Ncr}} \in]0, 1[$, which is assumed to be a constant of the model.

In our model, the coefficients ζ_{pn} , ζ_{nf} , ζ_{Np} and ζ_{fp} are constants, and can be related to the characteristic time scales with which, respectively, the proliferating cells die, the necrotic cells are converted into fluid, the nutrients are consumed and the interstitial fluid becomes a tumor due to cell growth.

We notice that the sinks defined in (31a)–(31d) depend on the solid phase volumetric fraction, $\varphi_{\text{s}} = (J_{\gamma} \Phi_{\text{sv}})/J$, in such a way that they vanish for vanishing φ_{s} . For the same reason, r_{pn} must be zero for zero ω_{p} , r_{Np} must be zero when ω_{p} or ω_{N} is zero, and r_{nf} must be zero for unitary ω_{p} , i.e., for zero ω_{n} (indeed, $\omega_{\text{n}} = 1 - \omega_{\text{p}}$). We remark, in addition, that the dependence of r_{Np} on ω_{N} is taken from Population Dynamics [69], with the constant $\omega_{\text{N0}} \in]0, 1[$ being a reference value of the nutrient concentration, introduced to modulate the rate at which their uptake occurs. The dependence of r_{fp} on φ_{s} and $\varphi_{\text{f}} = 1 - \varphi_{\text{s}}$ guarantees that growth ceases in the limit of compaction, i.e., when all the fluid flows away, and the porous medium features no voids, or when the solid disappears, which means that φ_{s} becomes zero. Besides, r_{fp} vanishes for vanishing ω_{p} , and is modulated by stress through the term $\langle \bar{\sigma} \rangle_+$, where $\bar{\sigma}$ is defined as

$$\bar{\sigma} = -\frac{1}{3}(\mathbf{g} : \boldsymbol{\sigma}_{\text{sc}}) = -\frac{\frac{2}{3} \sum_{i=1}^3 i b_i I_i}{J_{\text{e}}}. \quad (32)$$

We reserve now a separate treatment for the non-standard terms $r_{\text{p}\gamma}$ and $r_{\text{n}\gamma}$. In particular, for the sake of simplicity, we set $r_{\text{n}\gamma} = 0$ and we prescribe $r_{\text{p}\gamma}$ as,

$$r_{\text{p}\gamma} = c \left[\zeta_{\text{fp}} \frac{\omega_{\text{N}}}{\omega_{\text{Ncr}}} \frac{\varphi_{\text{f}} \varphi_{\text{s}}}{\varphi_{\text{f0}}} \omega_{\text{p}} \right] \kappa_{\gamma} = c \left[\zeta_{\text{fp}} \frac{\omega_{\text{N}}}{\omega_{\text{Ncr}}} \frac{J - J_{\gamma} \Phi_{\text{sv}}}{J \varphi_{\text{f0}}} \frac{J_{\gamma} \Phi_{\text{sv}}}{J} \omega_{\text{p}} \right] \kappa_{\gamma}. \quad (33)$$

502 With the formulation of $r_{p\gamma}$ given in (33), we assume that $r_{p\gamma}$ is proportional
503 to κ_γ through the factor $c \zeta_{fp}(\omega_N/\omega_{Ncr})(\varphi_f \varrho_s)/\varphi_{f0}$. In this work, the product
504 $c \zeta_{fp}$ is assumed to be constant and it represents, with respect to a suitable
505 time scale, the way in which the inhomogeneities induced by growth evolve
506 in the tissue. Moreover, as explained above for the standard terms (31a)–
507 (31d), we need to account for the limit cases in which compaction occurs
508 ($\varphi_f = 0$) or the solid phase is locally absent ($\varphi_s = 0$). In fact, we ensure
509 that $r_{p\gamma}$ vanishes when φ_f or φ_s vanish. Finally, we relate the availability of
510 nutrients to growth. In fact, we prescribe that growth does not take place if
511 $\omega_N = 0$, and we modulate the growth rate through the reference value ω_{Ncr} .
512 This factor, indeed, is introduced to re-scale the current mass fraction of the
513 nutrients, ω_N . In particular, the effect of κ_γ is amplified for $\omega_N > \omega_{Ncr}$, and
514 reduced for $\omega_N \leq \omega_{Ncr}$.

515 For the sake of a lighter exposition, in the present work we suppress the
516 rotations related to growth, so that \mathbf{R}_γ reduces to a shifter [61] from $T\mathcal{B}$
517 to $T\mathcal{N}_t$, and we assume that \mathbf{U}_γ represents a pure dilatation, i.e., we set
518 $\mathbf{U}_\gamma = \gamma \mathbf{I}$. This form of \mathbf{U}_γ also implies $J_\gamma = \gamma^3$ and $\mathbf{C}_\gamma = \gamma^2 \mathbf{G}$, so that the
519 material metric, \mathbf{G} , is rescaled by γ^2 . Hence, no remodelling is considered in
520 this work, and growth is entirely expressed in terms of an evolution law for
521 γ , which, for given r_{fp} and r_{nf} , coincides with (11b).

522 We emphasise that the introduction of κ_γ in our model of tumour growth
523 is the major novelty of our work, and it constitutes the principal difference
524 with respect to the model developed in [54]. The difference is in the fact
525 that, while (11b) is an ordinary differential equation in [54], it is a partial
526 differential equation in our model. This feature of our approach allows for
527 an explicit resolution of the spatial variability of γ and, more importantly,
528 it permits to estimate to what extent such variability influences growth. In
529 fact, going through the calculations leading to (6), we notice that κ_γ features
530 the derivatives of γ up to the second order. Hence, by introducing $r_{p\gamma}$ into
531 (11b), we obtain a nonlinear diffusion-reaction like equation in the unknown
532 γ . Solving this equation shows how the resolved spatial variability of γ
533 influences the evolution of the other model descriptors, i.e., the mass fraction
534 of the proliferating cells, the mass fraction of the nutrients, motion, and
535 pressure.

536 Looking at (11b), and combining it with the definitions (31b), (31d), and
537 (33), we notice that the just depicted situation is attained when the mass
538 fraction of the nutrients, ω_N , is below the threshold ω_{Ncr} (so that $r_{fp} = 0$),
539 i.e.,

$$\frac{\dot{\gamma}}{\gamma} = c \left[\frac{\zeta_{fp}}{3\varrho_s} \frac{\omega_N}{\omega_{Ncr}} \frac{\varphi_f}{\varphi_{f0}} \omega_p \right] \kappa_\gamma - \frac{\zeta_{nf}}{3\varrho_s} [1 - \omega_p]. \quad (34)$$

540 In (34), indeed, the evolution of γ is governed by an affine function of κ_γ ,
 541 and is modulated by the mass fractions ω_p and ω_N . More generally, instead,
 542 when ω_N is above ω_{Ncr} , Equation (34) becomes:

$$\begin{aligned} \frac{\dot{\gamma}}{\gamma} = & c \left[\frac{\zeta_{fp}}{3\varrho_s} \frac{\omega_N}{\omega_{Ncr}} \frac{\varphi_f}{\varphi_{f0}} \omega_p \right] \kappa_\gamma - \frac{\zeta_{nf}}{3\varrho_s} [1 - \omega_p] \\ & + \frac{\zeta_{fp}}{3\varrho_s} \left\langle \frac{\omega_N - \omega_{Ncr}}{\omega_{Nenv} - \omega_{Ncr}} \right\rangle_+ \left[1 - \frac{\delta_1 \langle \bar{\sigma} \rangle_+}{\delta_2 + \langle \bar{\sigma} \rangle_+} \right] \frac{\varphi_f}{\varphi_{f0}} \omega_p. \end{aligned} \quad (35)$$

543 Equation (35) combines two models: The first two terms on the right-hand-
 544 side of (35) are an adaptation of the model by Epstein [42] to our biphasic
 545 problem, which requires the introduction of the mass fraction of nutrients
 546 and proliferating cells as well as the volumetric fraction of the fluid phase.
 547 The last term, instead, is taken from the model by Mascheroni et al. [54] and
 548 has phenomenological nature in order to account for the fact that growth
 549 occurs when the mass fraction of the nutrients, ω_N , is greater than ω_{Ncr} , and
 550 it is modulated by stress.

551 **Remark 3.** Following [42], one could formulate a more general model, with-
 552 out the a priori assumptions of no growth-induced rotations and $\mathbf{U}_\gamma = \gamma \mathbf{I}$.
 553 In this case, a possible evolution law for \mathbf{F}_γ could be obtained by relating $\dot{\mathbf{F}}_\gamma$
 554 to a known function of \mathcal{R} and $\text{Grad} \mathcal{R}$. Such an evolution law, however, is
 555 out of the scope of this work. Therefore, for the moment, we simply neglect
 556 $\text{Grad} \mathcal{R}$ in the evolution law for \mathbf{F}_γ , thereby keeping only its derivatives up to
 557 the second order. Moreover, since in our framework it holds that $\mathbf{U}_\gamma = \gamma \mathbf{I}$,
 558 we end up with model in which the evolution of γ is a function of the scalar
 559 curvature, κ_γ , only.

560 4. Solution of a benchmark problem

561 4.1. Summary of the model

562 Before addressing the details of the considered benchmark problem, we
 563 summarise the model equations, and declare the unknowns to be determined.
 564 In doing this, we perform the following simplifications: (a) since the cells
 565 consist mainly of water, the mass densities ϱ_s and ϱ_f are regarded as equal
 566 to each other, so that the right-hand-side of (20a) is zero; (b) the advective
 567 term $\mathbf{Q} \text{Grad} \omega_N$ is considered to be negligible with respect to the other terms
 568 of (20a). In conclusion, the model equations are given by (11a), (11b), (20a),
 569 (20b), and (21), which we rewrite as

$$\text{Div} [-Jp\mathbf{g}^{-1} \mathbf{F}^{-T} + \mathbf{P}_{sc}] = \mathbf{0}, \quad (36a)$$

$$\dot{J} - \text{Div} [\mathbf{K} \text{Grad } p] = 0, \quad (36b)$$

$$(J - \gamma^3 \Phi_{s\nu}) \dot{\omega}_N - \text{Div} [\mathbf{D} \text{Grad } \omega_N] = J \left(\frac{r_{\text{Np}}}{\varrho_f} + \frac{3\gamma^3 \Phi_{s\nu} \omega_N}{J} \frac{\dot{\gamma}}{\gamma} \right), \quad (36c)$$

$$\dot{\omega}_p = -\frac{\zeta_{\text{pn}}}{\varrho_s} \left\langle 1 - \frac{\omega_N}{\omega_{\text{Ncr}}} \right\rangle_+ \omega_p + \frac{\zeta_{\text{nf}}}{\varrho_s} [1 - \omega_p] + 3[1 - \omega_p] \frac{\dot{\gamma}}{\gamma}, \quad (36d)$$

$$\frac{\dot{\gamma}}{\gamma} = c \left[\frac{\zeta_{\text{fp}}}{3\varrho_s} \frac{\omega_N}{\omega_{\text{Ncr}}} \frac{J - \gamma^3 \Phi_{s\nu}}{J - J\Phi_{s\nu}} \omega_p \right] \kappa_\gamma + \frac{J[r_{\text{fp}} + r_{\text{nf}}]}{3\gamma^3 \Phi_{s\nu} \varrho_s}, \quad (36e)$$

where r_{nf} , r_{Np} , and r_{fp} are defined in (31b), (31c), and (31d). Consistently with (36a)–(36e), the unknown of the models are the motion of the solid phase, χ , the pressure, p , the nutrient mass fraction, ω_N , the growth parameter, γ , and the mass fraction of the proliferating cells, ω_p . Finally, \mathbf{K} , \mathbf{D} , and \mathbf{P}_{sc} are specified in (23a), (23b), and (29), and all the material parameters are reported in Table 1 and in Table 2.

4.2. Description of the benchmark test

As a proof of concept, we specialise now Equations (36a)–(36e) to a benchmark problem taken from the literature. For our purposes, we select the problem of “*isotropic and homogeneous growth inside a rigid cylinder*”, formulated in [55] for the case of mono-phasic growing medium, and we adapt it to our scopes.

Also in our formulation the growth is isotropic, i.e., $\mathbf{U}_\gamma = \gamma \mathbf{I}$, and takes place inside a tissue specimen of cylindrical shape, with undeformable curved surface. Hence, both the reference and the current configurations of the tissue have cylindrical shapes, with equal radius and different lengths. We indicate by R_{in} and L the initial radius and the initial length of the cylinder, respectively. Moreover, the reference configuration is covered with a system of cylindrical coordinates $\hat{X} = (R, \Theta, Z)$, where R , Θ , and Z are the radial, circumferential, and axial coordinate, respectively. Analogously, the generic current configuration of the tissue is covered with the system of cylindrical coordinates $\hat{x} = (r, \vartheta, z)$. Any rigid rotation of the specimen about the axis of the cylinder is suppressed from the outset.

The restrictions imposed on χ imply that only the axial component of the momentum balance law (36a) has to be solved, and that the sole unknown component of the motion is the axial one, χ^z , while the radial and circumferential ones, χ^r and χ^ϑ , return the radial and the angular coordinate, respectively.

The growth cannot be assumed to be homogeneous in our framework, as the scalar curvature, κ_γ , would then be trivially zero, and our model would boil down to a simple biphasic rephrasing of the model presented in [55]. On

the contrary, to highlight the role of κ_γ , we prescribe initial distributions of γ with a strong gradient.

In [55], the two extremities of the considered cylinder are free of applied forces, so that the axial component of stress is zero both at two outermost sections of the cylinder and, because of homogeneity, everywhere else inside it. In our setting, however, we may only conclude that the overall axial Cauchy stress, $\sigma^{zz} = -p + \sigma_{sc}^{zz}$ is zero, whereas the pressure, p , and the constitutive Cauchy stress, σ_{sc}^{zz} , cannot be individually zero because of the point-dependent distribution of γ . In fact, they can be such only asymptotically, i.e., in the limit in which the initial inhomogeneities relax, and the conditions $p = 0$ and $\sigma_{sc}^{zz} = 0$ are the unique, stationary solutions to (36a) and (36b). Further differences with [55] are due to the different constitutive relations which we work with, and to the fact that our solid phase consists of two types of cells.

To solve (36a)–(36e) compatibly with the descriptions given so far, we prescribe the reference configuration of the tissue, \mathcal{B} , to be of cylindrical shape, and we assign the following set of boundary conditions, which apply for all times:

$$\chi^r = R_{\text{in}}, \quad \text{on } (\partial\mathcal{B})_{\text{C}}, \quad (37a)$$

$$\chi^\vartheta = \Theta, \quad \text{on } (\partial\mathcal{B})_{\text{C}}, \quad (37b)$$

$$(-Jp\mathbf{g}^{-1}\mathbf{F}^{-\text{T}} + \mathbf{P}_{\text{sc}}) \cdot \mathbf{N}_{\text{A}} = \mathbf{0}, \quad \text{on } (\partial\mathcal{B})_{\text{Left}} \text{ and } (\partial\mathcal{B})_{\text{Right}}, \quad (37c)$$

$$(-\mathbf{K}\text{Grad } p) \cdot \mathbf{N}_{\text{C}} = 0, \quad \text{on } (\partial\mathcal{B})_{\text{C}}, \quad (37d)$$

$$p = 0, \quad \text{on } (\partial\mathcal{B})_{\text{Left}} \text{ and } (\partial\mathcal{B})_{\text{Right}}, \quad (37e)$$

$$(-\varrho_{\text{f}}\mathbf{D}\text{Grad } \omega_{\text{N}}) \cdot \mathbf{N}_{\text{C}} = 0, \quad \text{on } (\partial\mathcal{B})_{\text{C}}, \quad (37f)$$

$$\omega_{\text{N}} = \omega_{\text{Nenv}}, \quad \text{on } (\partial\mathcal{B})_{\text{Left}} \text{ and } (\partial\mathcal{B})_{\text{Right}}, \quad (37g)$$

$$(\text{Grad } \gamma) \mathbf{N} = 0, \quad \text{on } \partial\mathcal{B}. \quad (37h)$$

In (37a)–(37g), $(\partial\mathcal{B})_{\text{C}}$ is the lateral boundary of the cylindric specimen, whereas $(\partial\mathcal{B})_{\text{Left}}$ and $(\partial\mathcal{B})_{\text{Right}}$ are the left and the right surfaces at the extremities of \mathcal{B} , respectively, \mathbf{N}_{A} is the unit vector field normal to $(\partial\mathcal{B})_{\text{Left}}$ and $(\partial\mathcal{B})_{\text{Right}}$, \mathbf{N}_{C} is the unit vector field oriented normal to $(\partial\mathcal{B})_{\text{C}}$, and R_{in} is the initial radius of the cylinder. Furthermore, it holds that $\partial\mathcal{B} = (\partial\mathcal{B})_{\text{Left}} \cup (\partial\mathcal{B})_{\text{Right}} \cup (\partial\mathcal{B})_{\text{C}}$, and \mathbf{N} is the unit vector field normal to $\partial\mathcal{B}$.

Before going further, we remark that the boundary conditions (37d) and (37f) describe the situation in which $(\partial\mathcal{B})_{\text{C}}$, besides being undeformable, is also impermeable to the fluid and to the nutrient. Finally, the Dirichlet condition (37g), with ω_{Nenv} kept constant in all calculations, means that the tissue specimen finds itself in a “bath” of nutrients, which can flow through the boundary surfaces $(\partial\mathcal{B})_{\text{Left}}$ and $(\partial\mathcal{B})_{\text{Right}}$.

631 Together with (37a)–(37g), we enforce the initial conditions:

$$\chi^r(R, \Theta, Z, 0) = R, \quad \chi^\vartheta(R, \Theta, Z, 0) = \Theta, \quad (38a)$$

$$\chi^z(R, \Theta, Z, 0) = Z + u_{\text{in}}(Z), \quad (38b)$$

$$p(R, \Theta, Z, 0) = 0, \quad (38c)$$

$$\omega_{\text{N}}(R, \Theta, Z, 0) = \omega_{\text{Nenv}}, \quad (38d)$$

$$\gamma(R, \Theta, Z, 0) = \gamma_{\text{in}}(Z), \quad (38e)$$

$$\omega_{\text{p}}(R, \Theta, Z, 0) = 1, \quad (38f)$$

632 which apply at all inner points of \mathcal{B} . The way in which the problem is
 633 formulated allows to infer that the deformation gradient tensor takes on
 634 the form $\mathbf{F} = \mathbf{e}_r \otimes \mathbf{E}^R + \mathbf{e}_\vartheta \otimes \mathbf{E}^\Theta + (1 + u')\mathbf{e}_z \otimes \mathbf{E}^Z$, where u is the axial
 635 displacement, the prime indicates partial differentiation in the axial direction
 636 (i.e., $u' \equiv \partial u / \partial Z$), while $\{\mathbf{e}_r, \mathbf{e}_\vartheta, \mathbf{e}_z\}$ and $\{\mathbf{E}^R, \mathbf{E}^\Theta, \mathbf{E}^Z\}$ are the vector basis
 637 and the co-vector basis generated by the coordinate systems $\hat{x} = (r, \vartheta, z)$ and
 638 $\hat{X} = (R, \Theta, Z)$, respectively. It is understood that $R \in [0, R_{\text{in}}]$, $\Theta \in [0, 2\pi[$,
 639 and $Z \in [-\frac{1}{2}L, \frac{1}{2}L]$.

640 As a further simplification, we require that all the physical quantities
 641 involved in the model are point-independent on each cross-section of the
 642 specimen, whereas they *do* vary along the axis of the cylinder, i.e., they are
 643 point-dependent only through the axial coordinate, Z . Therefore, the scalar
 644 curvature reads

$$\kappa_\gamma = \frac{2(\gamma')^2 - 4\gamma\gamma''}{\gamma^4} = \frac{6(\gamma')^2 - (4\gamma\gamma')'}{\gamma^4}, \quad (39)$$

645 and the model equations simplify as reported below:

$$[(\mathbf{P}_{\text{sc}})^{zZ}]' = p', \quad (40a)$$

$$\frac{\dot{\cdot}}{1 + u'} = \left[\frac{k_0}{1 + u'} p' \right]', \quad (40b)$$

$$\begin{aligned} [(1 + u') - \gamma^3 \Phi_{s\nu}] \dot{\omega}_{\text{N}} &= \left[\left(\frac{(1 + u') - \gamma^3 \Phi_{s\nu}}{(1 + u')^2} d_{0\text{R}} \right) \omega'_{\text{N}} \right]' \\ &\quad + \gamma^3 \Phi_{s\nu} \left[3 \frac{\dot{\gamma}}{\gamma} \omega_{\text{N}} - \frac{\zeta_{\text{Np}}}{\varrho_{\text{f}}} \frac{\omega_{\text{N}}}{\omega_{\text{N}} + \omega_{\text{N0}}} \omega_{\text{p}} \right], \end{aligned} \quad (40c)$$

$$\dot{\omega}_{\text{p}} = -\frac{\zeta_{\text{pn}}}{\varrho_{\text{s}}} \left\langle 1 - \frac{\omega_{\text{N}}}{\omega_{\text{Ncr}}} \right\rangle_+ \omega_{\text{p}} + \frac{\zeta_{\text{nf}}}{\varrho_{\text{s}}} [1 - \omega_{\text{p}}] + 3[1 - \omega_{\text{p}}] \frac{\dot{\gamma}}{\gamma}, \quad (40d)$$

$$\frac{\dot{\gamma}}{\gamma} = |c| \left[\frac{\zeta_{\text{fp}}}{3\varrho_{\text{s}}} \frac{\omega_{\text{N}}}{\omega_{\text{Ncr}}} \frac{(1 + u') - \gamma^3 \Phi_{s\nu}}{(1 + u')(1 - \Phi_{s\nu})} \omega_{\text{p}} \right] \frac{4\gamma\gamma'' - 2(\gamma')^2}{\gamma^4}$$

$$\begin{aligned}
& + \frac{\zeta_{\text{fp}}}{3\rho_s} \left\langle \frac{\omega_{\text{N}} - \omega_{\text{Ncr}}}{\omega_{\text{Nenv}} - \omega_{\text{Ncr}}} \right\rangle_+ \left[1 - \frac{\delta_1 \langle \bar{\sigma} \rangle_+}{\delta_2 + \langle \bar{\sigma} \rangle_+} \right] \frac{(1 + u') - \gamma^3 \Phi_{s\nu}}{(1 + u')(1 - \Phi_{s\nu})} \omega_{\text{p}} \\
& - \frac{\zeta_{\text{nf}}}{3\rho_s} [1 - \omega_{\text{p}}],
\end{aligned} \tag{40e}$$

646 where we have set $J = 1 + u'$, and k_0 is defined in (22a). Equations (40a)–
 647 (40d) are now put in weak form, and solved by employing the Finite Element
 648 Method. To eliminate rigid motions along the axial direction, we introduce
 649 a Dirichlet point for u at $Z = 0$, where we prescribe $u(0, t) = 0$ for all t .
 650 Finally, we assign the initial conditions $\gamma_{\text{in}}(Z)$ and $u_{\text{in}}(Z)$ in such a way that
 651 the problem results to be symmetric with respect to $Z = 0$.

Parameter	Unit	Value	Equation	Reference
L	[cm]	1.000	Initial length	—
R_{in}	[cm]	$1.000 \cdot 10^{-2}$	Initial radius	—
λ	[Pa]	$1.333 \cdot 10^4$	(27)	[70]
μ	[Pa]	$1.999 \cdot 10^4$	(27)	[70]
k_0	[mm ⁴ /(N s)]	0.4875	(22a), (23a),	[66]
m_0	[—]	0.0848	(22a)	[66]
m_1	[—]	4.638	(22a)	[66]
$d_{0\text{R}}$	[m ² /s]	$3.200 \cdot 10^{-9}$	(22b), (40c)	[66]

Table 1: Parameters used in the definitions of the energy density, permeability and diffusivity. The mass fraction of the solid phase in the natural state is $\Phi_{s\nu} = 0.8$. The solid and fluid phase densities are $\rho_s = \rho_f = 1000 \text{ kg/m}^3$.

652 5. Results

653 To evaluate the impact of the scalar curvature, κ_γ , on the evolution of
 654 the system under study, we solve (40a)–(40e) twice: First, we set $c = 0$ in
 655 (40e), thereby switching off the term with κ_γ (this first model is denominated
 656 M1). Then, we set $c \neq 0$, and solve (40a)–(40e), paying particular attention
 657 to the effect of κ_γ (this second model is referred to as M2).

658 For our purposes, we prepare a protocol of numerical experiments in which
 659 the initial distribution of the growth-related distortions, $\gamma_{\text{in}}(Z)$, has strong
 660 gradients and non-vanishing curvatures. Specifically, we consider two types
 661 of $\gamma_{\text{in}}(Z)$, i.e.,

$$\gamma_{\text{osc}}(Z) = f_0 + g_0 \cos(h_0 Z), \tag{41a}$$

$$\gamma_{\text{atan}}(Z) = \begin{cases} a_0 - b_0 \operatorname{atan}(r_0 (Z + \frac{1}{4}L)), & Z \in [-\frac{1}{2}L, 0], \\ a_0 + b_0 \operatorname{atan}(r_0 (Z - \frac{1}{4}L)), & Z \in]0, \frac{1}{2}L], \end{cases} \tag{41b}$$

Parameter	Unit	Value	Description	Reference
ζ_{fp}	$[\text{kg}/(\text{m}^3 \text{ s})]$	$1.343 \cdot 10^{-3}$	(31d), (33), (42)	[71]
ζ_{pn}	$[\text{kg}/(\text{m}^3 \text{ s})]$	$1.500 \cdot 10^{-3}$	(31a)	[71]
ζ_{nf}	$[\text{kg}/(\text{m}^3 \text{ s})]$	$1.150 \cdot 10^{-5}$	(31b)	[71]
ζ_{Np}	$[\text{kg}/(\text{m}^3 \text{ s})]$	$3.000 \cdot 10^{-4}$	(31c)	[72, 73]
c	$[\text{m}^2]$	$\{0, -10^{-6}\}$	(33)	—
g_0	$[-]$	$0.125 \cdot 10^{-1}$	(41a)	—
f_0	$[-]$	$1 + g_0$	(41a)	—
h_0	$[\text{1/cm}]$	8π	(41a)	—
a_0	$[-]$	1.020	(41b)	—
b_0	$[-]$	0.010	(41b)	—
r_0	$[\text{1/cm}]$	50π	(41b)	—
ω_{Ncr}	$[-]$	$1.000 \cdot 10^{-3}$	(31d), (33), (42)	—
ω_{Nenv}	$[-]$	$7.000 \cdot 10^{-3}$	(31d), (42)	—
ω_{N0}	$[-]$	$1.480 \cdot 10^{-4}$	(31c)	—
δ_1	$[-]$	$7.138 \cdot 10^{-1}$	(31d), (42)	[74]
δ_2	$[\text{Pa}]$	$1.541 \cdot 10^3$	(31d), (42)	[74]

Table 2: Parameters used in the definitions of the system’s geometry, in the definitions of the sources and sinks of mass, and in the initial conditions for γ .

both defining even functions with respect to $Z = 0$, and representing a grown configuration of the tumour characterised by strong inhomogeneities. All the parameters featuring in (41a) and (41b) are reported in Table 2. The models ‘M1’ and ‘M2’ are further specialised in ‘M1(a)’ and ‘M2(a)’, for $\gamma_{\text{in}} = \gamma_{\text{osc}}$, and ‘M1(b)’ and ‘M2(b)’, for $\gamma_{\text{in}} = \gamma_{\text{atan}}$.

5.1. Formulation of specialised sub-models

Models M1(a) and M1(b) [no spatial resolution of the inhomogeneities]. We solve (40a)–(40e) with $c = 0$, thereby switching off the curvature in the simulations. Hence, (40e) reduces to the ordinary differential equation

$$\begin{aligned} \frac{\dot{\gamma}}{\gamma} = & \frac{\zeta_{\text{fp}}}{3\varrho_{\text{s}}} \left\langle \frac{\omega_{\text{N}} - \omega_{\text{Ncr}}}{\omega_{\text{Nenv}} - \omega_{\text{Ncr}}} \right\rangle_+ \left[1 - \frac{\delta_1 \langle \bar{\sigma} \rangle_+}{\delta_2 + \langle \bar{\sigma} \rangle_+} \right] \frac{(1 + u') - \gamma^3 \Phi_{s\nu}}{(1 + u')(1 - \Phi_{s\nu})} \omega_{\text{p}} \\ & - \frac{\zeta_{\text{nf}}}{3\varrho_{\text{s}}} [1 - \omega_{\text{p}}], \end{aligned} \quad (42)$$

and the boundary condition (37h) is no longer necessary. Therefore, together with (40a)–(40d) and (42), only the boundary conditions (37a)–(37g) and the initial conditions (38a)–(38f) have to be accounted for.

Although the spatial variability of γ does not play a direct role on (42), the initial distribution of the growth-related distortions *does* influence the evolution of γ .

Models $M2(a)$ and $M2(b)$ [spatial resolution of the inhomogeneities]. We solve (40a)–(40e) with $c \neq 0$, and we enforce the complete set of boundary and initial conditions, i.e., (37a)–(37h) and (38a)–(38f), respectively. In this case, the scalar curvature, κ_γ , does contribute to drive the evolution of γ , through the first term on the right-hand-side of (40e).

5.2. Numerical results

In Fig. 2, we report the displacement of the tumour in the axial direction of the specimen, evaluated at the cross section of the cylinder $Z = L/2$, i.e., $u(L/2, t) = \chi^z(L/2, t) - \chi^z(L/2, 0)$. As expected, in all the considered cases, the results of our simulations show that $u(L/2, t)$ increases monotonically with time. By comparing M1(a) with M2(a), and M1(b) with M2(b), we note that the curvature seems to play a significant role in the evolution of the tumour displacement. In fact, the inclusion of the curvature augments the steepness of the displacement from the beginning of the simulation, and, from the 3rd day onward, it increases its magnitude appreciably. This result suggests, in addition, that the initial inhomogeneities do relax, and that the system, at the end of the simulation, finds itself in a homogeneous configuration. These deductions are confirmed by Fig. 3 and Fig. 4, in which the spatial distribution of the scalar curvature κ_γ , at the initial and final instants of time, is presented.

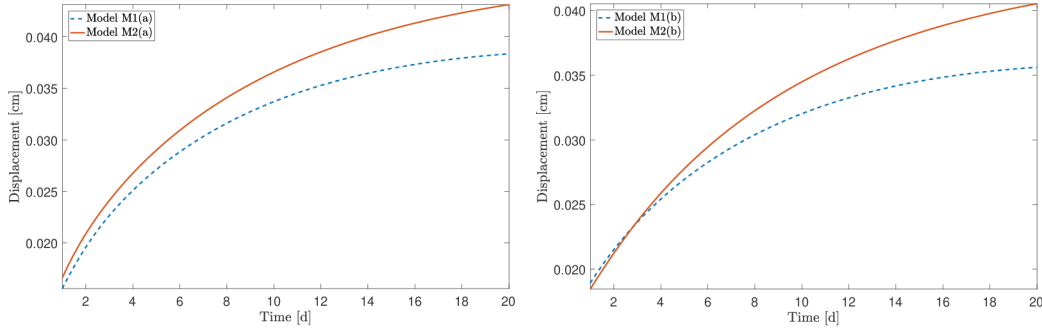


Figure 2: Evolution of the tumour in the axial direction, evaluated at the cross section $Z = L$. Panel on the left: comparison between M1(a) and M2(a), for which $\gamma_{\text{in}} = \gamma_{\text{osc}}$. Panel on the right: comparison between M1(b) and M2(b), for which $\gamma_{\text{in}} = \gamma_{\text{atan}}$.

Starting from Fig. 3, we note that the oscillating behaviour of the scalar curvature κ_γ , which reflects the trend of the initial distribution of the inhomogeneities $\gamma_{\text{in}} = \gamma_{\text{osc}}$, results strongly mitigated at the end of the simulation. In fact, no oscillation can be appreciated in this case, and κ_γ is closer to zero than the initial case, which means that tissue is evolving towards a homogeneous configuration. Analogously, in Fig. 4, the concentration of the gradient,

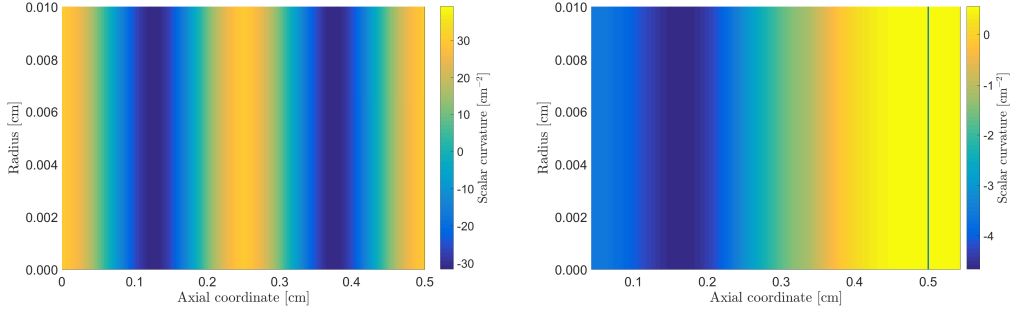


Figure 3: Spatial distribution of the scalar curvature κ_γ evaluated on the meridian section of the specimen, in the case of $\gamma_{\text{in}} = \gamma_{\text{osc}}$. Panel on the left: initial instant of time. Panel on the right: final instant of time.

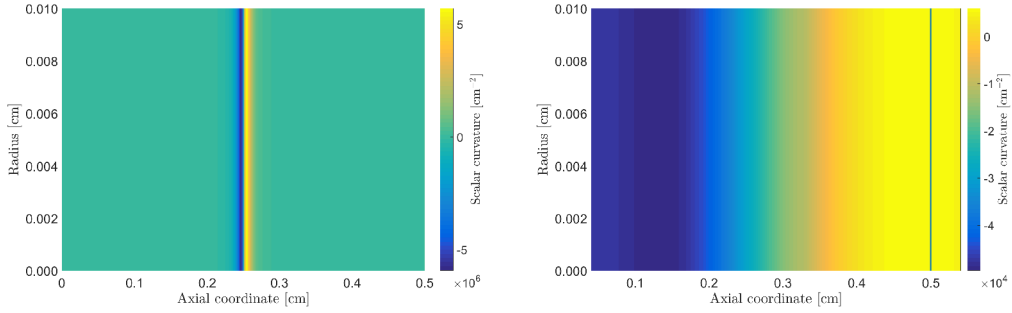


Figure 4: Spatial distribution of the scalar curvature κ_γ evaluated on the meridian section of the specimen, in the case of $\gamma_{\text{in}} = \gamma_{\text{atan}}$. Panel on the left: initial instant of time. Panel on the right: final instant of time.

703 which characterizes the scalar curvature for the model with $\gamma_{\text{in}} = \gamma_{\text{osc}}$, re-
 704 laxes at the end of the simulation. Also in this case, the tissue attains a
 705 final configuration in which the inhomogeneities are appreciably appeased.
 706 The presence of the curvature κ_γ in the model and its relaxation, influences
 707 the spatial trend of the growth. In this sense, looking at Fig. 5, we notice
 708 that marked qualitative differences emerge among the spatial profiles of γ
 709 computed with M1(a) and M2(a), or M1(b) and M2(b). Still, if we neglect
 710 the embodiment of the curvature, the curves are qualitatively similar, with
 711 the magnitude increasing as time goes by. In particular, no peculiarity of
 712 the initial data seems to be found in the computed curves: The presence
 713 of oscillations in the case for which $\gamma_{\text{in}} = \gamma_{\text{osc}}$ (left), or the steep change in
 714 concavity, for the other choice of γ_{in} , i.e. $\gamma_{\text{in}} = \gamma_{\text{atan}}$ (right). On the other
 715 hand, when the curvature is explicitly considered, the spatial distribution
 716 of the growth is strongly influenced by the initial conditions. In detail, de-
 717 pending on time, the oscillations (left) and the rapid change in concavity

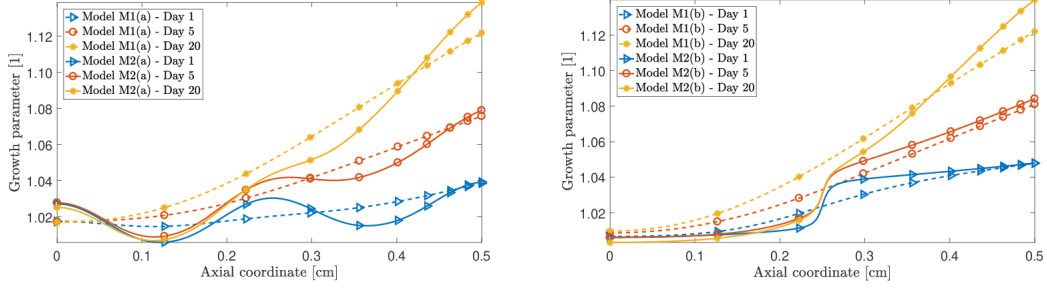


Figure 5: Spatial profile of the growth parameter γ for the models with $\gamma_{\text{in}} = \gamma_{\text{osc}}$ (panel on the left) and $\gamma_{\text{in}} = \gamma_{\text{atan}}$ (panel on the right). Since the problem is symmetric, only the half $[0, L/2]$ of the domain is shown.

(right), characterizing the two chosen initial distribution of inhomogeneities, are mitigated, but still present, until the end of the simulations. Although the differences outlined above, and independently on the initial condition γ_{in} , all the considered models lead to a final spatial behaviour of γ , in which the inhomogeneities are present.

Another point to put in evidence concerns Fig. 5(left). The sub-system corresponding to the interval $[0, L/2]$ is initially symmetric with respect to $Z = L/4$. Yet, this further symmetry is lost in the course of time, as visible from the the spatial profile of γ . This peculiarity of the results could be explained by referring to biological motivations, rather than geometric ones. To specify this aspect, let us focus on Fig. 6, which reports the trend of the nutrient mass fraction. We note, indeed, that the nutrients tend to diffuse from the boundaries $(\partial\mathcal{B})_{\text{Left}}$ and $(\partial\mathcal{B})_{\text{Right}}$ towards the centre of the specimen, along its axial direction. In the course of this process, there exists an instant of time after which the mass fraction of the nutrients becomes smaller than the critical value ω_{Ncr} in the interior of the tumour. Hence, while the growth of the tumour is inhibited in its centre, it is active close to the free boundaries, where the mass fraction of the nutrients is still higher than the critical threshold.

A relevant result concerns the dynamics of the proliferating cells, as shown in Fig. 7. Their mass fraction, ω_p , remains close to unity in the proximity of the boundary $(\partial\mathcal{B})_{\text{Right}}$, where the level of nutrients is still high, while it diminishes in the centre of the tumour, where nutrients tend to become unavailable (this means that the proliferating cells are “converted” into necrotic ones). This phenomenon is influenced by the explicit resolution of the curvature in the model. Indeed, when the curvature is explicitly considered, the conversion process of proliferating cells into necrotic ones is accelerated in the first days, and slowed down towards the end of the simulations. This behaviour occurs for both choices of γ_{in} , but appears to be slightly more

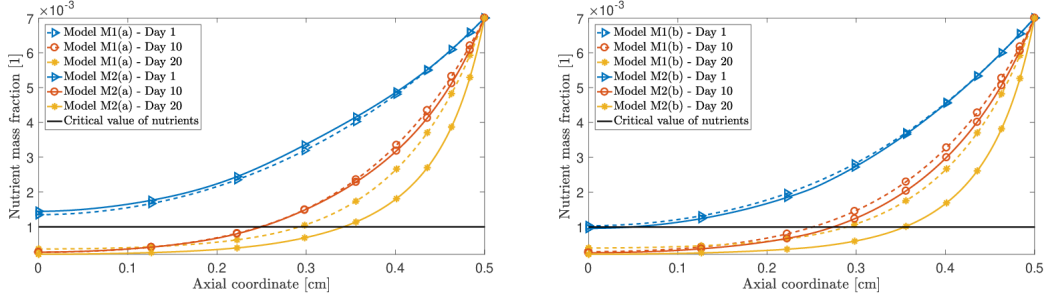


Figure 6: Spatial profile of the nutrients mass fraction ω_N for the models with $\gamma_{in} = \gamma_{osc}$ (panel on the left) and $\gamma_{in} = \gamma_{atan}$ (panel on the right). Since the problem is symmetric, only the half $[0, L/2]$ of the domain is shown.

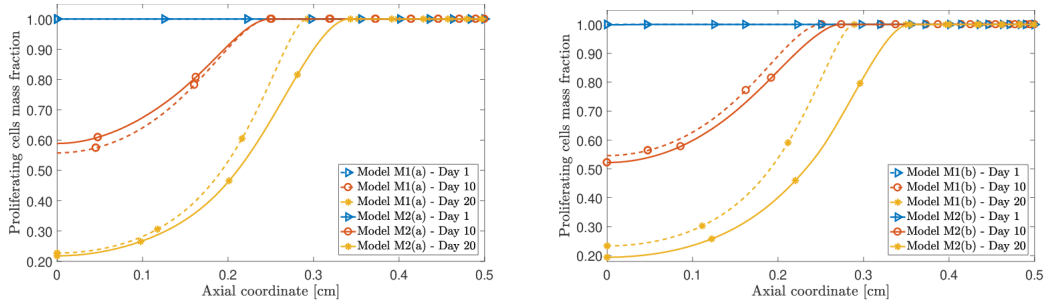


Figure 7: Spatial profile of the proliferants mass fraction ω_P for the models with $\gamma_{in} = \gamma_{osc}$ (panel on the left) and $\gamma_{in} = \gamma_{atan}$ (panel on the right). Since the problem is symmetric, only the half $[0, L/2]$ of the domain is shown.

747 pronounced for $\gamma_{in} = \gamma_{atan}$.

748 To proceed with our analysis, we refer to Fig. [8](#), where we plot the be-
 749 haviour of the pressure, p . When the tumour grows, the interstitial fluid flows
 750 towards the centre of the tumour, and p decreases from the free boundary
 751 (where the condition $p = 0$ applies) to the tumour's interior, where it takes
 752 on negative values. However, when the system goes towards the end of the
 753 simulations, p tends to become positive in the cases in which the curvature
 754 is explicitly accounted for, while it tends to zero from below otherwise.

755 Finally, in Fig. [9](#), we display the effective stress $\bar{\sigma}$. First, we notice that
 756 the tumour is subjected to a compressive stress, since $\bar{\sigma}$ is positive. Apart
 757 from this result, which is common to all the studied cases, we report that the
 758 curvature modifies the qualitative behaviour of $\bar{\sigma}$. As final remark, we note
 759 how the spatial evolution of the stress in the specimen, independently of the
 760 model, is strongly affected by the initial distribution of the inhomogeneities.

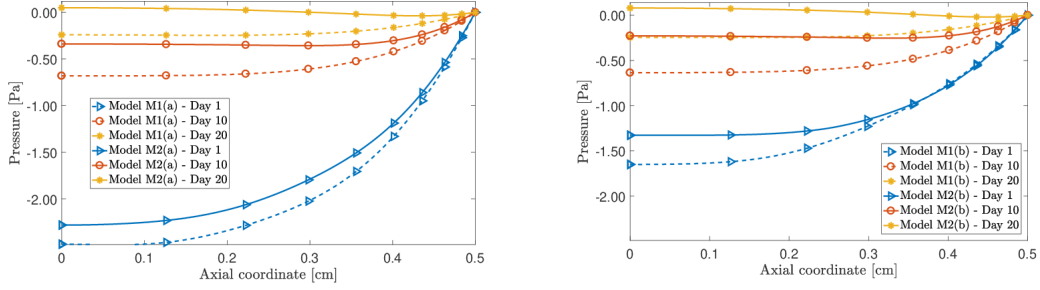


Figure 8: Spatial profile of the pore pressure p for the models with $\gamma_{in} = \gamma_{osc}$ (panel on the left) and $\gamma_{in} = \gamma_{atan}$ (panel on the right). Since the problem is symmetric, only the half $[0, L/2]$ of the domain is shown.

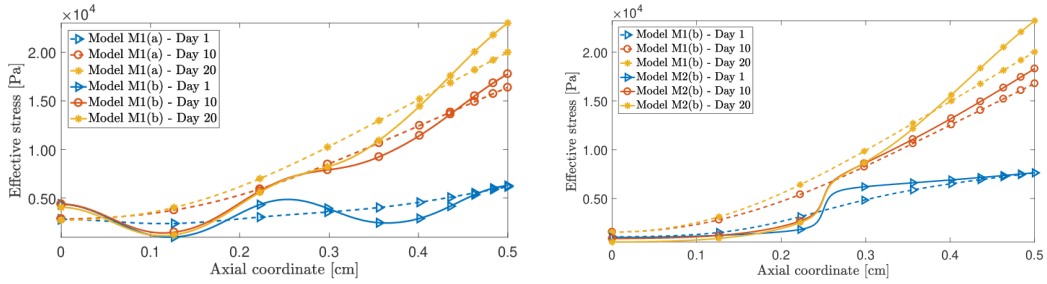


Figure 9: Spatial profile of the effective stress $\bar{\sigma}$ for the models with $\gamma_{in} = \gamma_{osc}$ (panel on the left) and $\gamma_{in} = \gamma_{atan}$ (panel on the right). Since the problem is symmetric, only the half $[0, L/2]$ of the domain is shown.

6. Conclusion

In this work, a mathematical model addressing tumour growth has been presented. The mechanical framework has been developed by regarding the tumour as a multi-constituent, biphasic medium, and by enforcing the BKL-decomposition of the deformation gradient tensor. The growth of the tumour is influenced by both mechanical stimuli and biological factors, such as the nutrients transported by the interstitial fluid, and the interactions among proliferating and necrotic cells.

The principal novelty of our approach consists of a partial reformulation of the balance laws for the constituents of the solid phase, in such a way that it is introduced an explicitly dependence on the scalar curvature, κ_γ , generated by the growth tensor $\mathbf{U}_\gamma = \gamma \mathbf{I}$ through the Riemannian, growth-related metric tensor $\mathbf{C}_\gamma = \gamma^2 \mathbf{G}$.

The introduction of κ_γ amounts to express the evolution law for γ as a partial differential equation, with the purpose of obtaining a better resolution of the material inhomogeneities, and an estimate of their influence on growth. To accomplish this task, we prescribe two types of initial conditions for γ ,

778 both characterised by strong gradients and nonzero initial curvature, $\kappa_{\gamma_{\text{in}}}$.

779 Two more thoughts about our results may be worth to be mentioned. The
 780 first one concerns the physical interpretation of the relaxation of the initial
 781 inhomogeneities accompanying γ_{in} . Indeed, since γ evolves according to a
 782 generalised diffusion-reaction like equation, one may say that, in our model,
 783 the material inhomogeneities brought about by growth “dissipate” towards
 784 a configuration in which they are spread over the tissue. The second thought
 785 pertains to the structure of the evolution equation (40e), and is also related
 786 to the first one. Indeed, by relaxing the initial inhomogeneities, the system
 787 tends to pass from a configuration in which it is not invariant under mate-
 788 rial translations to a homogeneous configuration in which it is translational
 789 invariant, thereby restoring the symmetry that is initially broken by γ_{in} .

790 One limitation of our study is related to the fact that, in this work, we
 791 have just relied on a phenomenological model in which κ_{γ} appears without a
 792 strong theoretical justification. We have not built a systematic constitutive
 793 framework, in which, for example, the strain energy density of our material
 794 depends on γ *and* on κ_{γ} , nor have we conducted any study of the Dissipation
 795 Inequality of the system at hand. Yet, confident in the intuitions that have
 796 led to the model presented in [42], we hope that our results could provide a
 797 basis for further investigations.

798 In our work, we concentrated on an academic benchmark problem in order
 799 to compare our results with those of other Authors and, in particular, with
 800 those of Ambrosi and Mollica [55]. For this reason, our general setting is *as*
 801 simple *as* the setting of the problems taken as reference, expect for the fact
 802 that we deal with a biphasic system featuring two cell populations and for the
 803 fact that we account for the role of inhomogeneities through the introduction
 804 of the term $r_{p\gamma}$ in the mass balance law of the proliferant cells. Clearly, our
 805 model can be further generalised and, in our opinion, this could be done in
 806 several steps. Here, we give some indications on how the formulation of our
 807 problem should look like if such generalisations were done.

808 First, one could consider exactly the same framework and geometry as
 809 the ones presented here, while relaxing the hypothesis of axial symmetry
 810 of the problem. In this case, the initial inhomogeneities may vary not only
 811 in the axial direction, but also radially or circumferentially, and the scalar
 812 curvature κ_{γ} must be computed according to its own definition (6), since it
 813 is no longer represented by (39). This requires the computation of all the
 814 partial derivatives necessary to determine the Christoffel symbols as well as
 815 the fourth-order curvature tensor specified in (4) and (5), respectively.

816 A second option could be to formulate an evolution law for γ in which the
 817 evolution is driven by the full curvature tensor \mathcal{R} and its gradient $\text{Grad}\mathcal{R}$,
 818 rather than by the scalar curvature only. In this case, the definitions of $r_{p\gamma}$

819 and $r_{n\gamma}$ should be further generalised, thereby implying a rewriting of the
820 mass balance laws of the proliferant and necrotic cells.

821 A further extension of the model could be the formulation of an evolution
822 law for the whole growth tensor \mathbf{F}_γ , with a restriction on $\text{tr}[\dot{\mathbf{F}}_\gamma \mathbf{F}_\gamma^{-1}]$, as done
823 in (10b). A model of this type extends the concept of growth presented in
824 this work and further rephrases the theory proposed in [42].

825 Another step is to specialise our model to problems with more realistic
826 geometries, which may arise from two- and three-dimensional studies. For a
827 given study, this means that the boundary value problem formulated in our
828 work has to be modified, and the Finite Element scheme adopted to solve it
829 have to be extended accordingly. In particular, the use of new computational
830 schemes may not be needed to resolve physical phenomena that could not be
831 captured otherwise, as is the case, for example, when the growth of a tumour
832 in the present of a host tissue and is studied [54].

833 Finally, although in the present work we dispensed with remodelling from
834 the outset, we are aware of the fact that such process accompanies growth.
835 In fact, it plays an important role in the redistribution of the mechanical
836 stress within the tissue and, thus, on the modulating effect of the latter on
837 the growth of a tumour. One possible way for studying remodelling is to use
838 the decompositions $\mathbf{F} = \mathbf{F}_e \mathbf{F}_r \mathbf{F}_\gamma$ or as $\mathbf{F} = \mathbf{F}_e \mathbf{F}_\gamma \mathbf{F}_r$, where \mathbf{F}_r represents
839 the distortion tensor describing the remodelling process, and to study the
840 dynamics of \mathbf{F}_r in relationship with all the other model variables. In the
841 literature, \mathbf{F}_r is often assumed to be a plastic-like phenomenon and is thus
842 treated accordingly. Within the context of tumour growth, \mathbf{F}_r accounts for
843 the structural transformations of a tissue at the cellular level. Its introduction
844 requires to elaborate numerical schemes capable of capturing the interplay
845 between the growth and the structural evolution of a tissue, even when these
846 phenomena exhibit rather separated time scales.

847 Moreover, our model could be developed and extended to describe other
848 biological situations. For instance, the approach presented in this work for
849 isotropic media could be adapted for describing a tumour growing in anisotropic
850 tissues. Moreover, we could investigate the coupling with remodelling phe-
851 nomena, introduced in term of cellular reorganisation, or the onset of degen-
852 erative phenomena. Finally, at the pore scale, the effect of inhomogeneities
853 could be studied by introducing a kinematic descriptor, called “*intrinsic vol-
854 ume ratio*” [64].

855 Conflict of Interests

856 The Authors declare that they have no conflict of interests.

857 **Acknowledgments**

858 We thank Prof. Marcelo Epstein (The University of Calgary, Canada) for
859 proficuous discussions, which helped us in the understanding of his work.

860 **References**

861 **References**

- 862 [1] R. P. Araujo, D. L. McElwain, A history of the study of solid tumour
863 growth: the contribution of mathematical modelling, Bulletin of Math-
864 ematical Biology [doi:10.1016/s0092-8240\(03\)00126-5](https://doi.org/10.1016/s0092-8240(03)00126-5).
- 865 [2] T. Alarcón, H. Byrne, P. Maini, A cellular automaton model for tumour
866 growth in inhomogeneous environment, Journal of Theoretical Biology
867 225 (2) (2003) 257–274. [doi:10.1016/s0022-5193\(03\)00244-3](https://doi.org/10.1016/s0022-5193(03)00244-3).
- 868 [3] G. W. Jones, S. J. Chapman, Modeling growth in biological materials,
869 SIAM Review 54 (1) (2012) 52–118. [doi:10.1137/080731785](https://doi.org/10.1137/080731785).
- 870 [4] A. Guerra, D. Rodriguez, S. Montero, J. Betancourt-Mar, R. Martin,
871 E. Silva, M. Bizzarri, G. Cocho, R. Mansilla, J. Nieto-Villar, Phase tran-
872 sitions in tumor growth VI: Epithelial–mesenchymal transition, Phys-
873 ica A: Statistical Mechanics and its Applications 499 (2018) 208–215.
874 [doi:10.1016/j.physa.2018.01.040](https://doi.org/10.1016/j.physa.2018.01.040).
- 875 [5] N. Bellomo, L. Preziosi, Modelling and mathematical problems re-
876 lated to tumor evolution and its interaction with the immune sys-
877 tem, Mathematical and Computer Modelling 32 (3-4) (2000) 413–452.
878 [doi:10.1016/s0895-7177\(00\)00143-6](https://doi.org/10.1016/s0895-7177(00)00143-6).
- 879 [6] H. M. Byrne, M. A. Chaplain, Growth of nonnecrotic tumors in the
880 presence and absence of inhibitors., Mathematical biosciences 130 (1995)
881 151–181.
- 882 [7] H. Byrne, D. Drasdo, Individual-based and continuum models of growing
883 cell populations: a comparison, Journal of Mathematical Biology 58 (4-
884 5) (2009) 657–687. [doi:10.1007/s00285-008-0212-0](https://doi.org/10.1007/s00285-008-0212-0).
- 885 [8] P. Macklin, S. McDougall, A. R. A. Anderson, M. A. J. Chaplain,
886 V. Cristini, J. Lowengrub, Multiscale modelling and nonlinear simula-
887 tion of vascular tumour growth, Journal of Mathematical Biology 58 (4-
888 5) (2009) 765–798. [doi:10.1007/s00285-008-0216-9](https://doi.org/10.1007/s00285-008-0216-9).

- [9] T. Roose, S. J. Chapman, P. K. Maini, Mathematical models of avascular tumor growth, *SIAM Review* 49 (2) (2007) 179–208. [doi:10.1137/S0036144504446291](https://doi.org/10.1137/S0036144504446291).
- [10] D. Ambrosi, G. Ateshian, E. Arruda, et al., Perspectives on biological growth and remodeling, *J. Mech. Phys. Solids* 59(4) (2011) 863–883. [doi:10.1016/j.jmps.2010.12.011](https://doi.org/10.1016/j.jmps.2010.12.011).
- [11] J. D. Humphrey, Towards a theory of vascular growth and remodeling, in: H. G.A., O. R.W. (Eds.), *Mechanics of Biological Tissue*, Springer-Verlag, 2006, pp. 3–15. [doi:10.1007/3-540-31184-x_1](https://doi.org/10.1007/3-540-31184-x_1).
- [12] H. Byrne, L. Preziosi, Modelling solid tumour growth using the theory of mixtures, *Mathematical Medicine and Biology* 20 (4) (2003) 341–366. [doi:10.1093/imamb/20.4.341](https://doi.org/10.1093/imamb/20.4.341).
- [13] L. Preziosi, G. Vitale, A multiphase model of tumor and tissue growth including cell adhesion and plastic reorganization, *Math. Models Methods Appl. Sci.* 21 (09) (2011) 1901–1932. [doi:10.1142/S0218202511005593](https://doi.org/10.1142/S0218202511005593).
- [14] D. Ambrosi, L. Preziosi, G. Vitale, The insight of mixtures theory for growth and remodeling, *Z. Angew. Math. Phys.* 61 (2010) 177–191. [doi:10.1007/s00033-009-0037-8](https://doi.org/10.1007/s00033-009-0037-8).
- [15] A. Grillo, S. Federico, G. Wittum, Growth, mass transfer, and remodeling in fiber-reinforced, multi-constituent materials, *Int. J. Nonlinear Mech.* 47 (2012) 388–401. [doi:10.1016/j.ijnonlinmec.2011.09.026](https://doi.org/10.1016/j.ijnonlinmec.2011.09.026).
- [16] G. Ateshian, J. Humphrey, Continuum mixture models of biological growth and remodeling: Past successes and future opportunities, *Annual Review of Biomedical Engineering* 14 (1) (2012) 97–111. [doi:10.1146/annurev-bioeng-071910-124726](https://doi.org/10.1146/annurev-bioeng-071910-124726).
- [17] R. D. O’Dea, S. L. Waters, H. M. Byrne, A multiphase model for tissue construct growth in a perfusion bioreactor, *Mathematical Medicine and Biology* 27 (2) (2010) 95–127. [doi:10.1093/imamb/dqp003](https://doi.org/10.1093/imamb/dqp003).
- [18] D. Ambrosi, S. Pezzuto, D. Riccobelli, T. Stylianopoulos, P. Ciarletta, Solid tumors are poroelastic solids with a chemo-mechanical feedback on growth, *J. Elast.* 129 (2017) 107–124. [doi:10.1007/s10659-016-9619-9](https://doi.org/10.1007/s10659-016-9619-9).

- [19] A. DiCarlo, S. Quiligotti, Growth and balance, *Mechanics Research Communications* 29 (6) (2002) 449–456. [doi:10.1016/s0093-6413\(02\)00297-5](https://doi.org/10.1016/s0093-6413(02)00297-5).
- [20] S. C. Cowin, G. A. Holzapfel, On the modeling of growth and adaptation, in: H. G. A., O. R. W. (Eds.), *Mechanics of Biological Tissue*, Springer-Verlag, 2006, pp. 29–46. [doi:10.1007/3-540-31184-x_3](https://doi.org/10.1007/3-540-31184-x_3).
- [21] A. Guillou, R. W. Ogden, Growth in soft biological tissue and residual stress development, in: G. Holzapfel, R. Ogden (Eds.), *Mechanics of Biological Tissue*, Springer-Verlag, 2006, pp. 47–62. [doi:10.1007/3-540-31184-x_4](https://doi.org/10.1007/3-540-31184-x_4).
- [22] G. A. Ateshian, On the theory of reactive mixtures for modeling biological growth, *Biomechanics and Modeling in Mechanobiology* 6 (6) (2007) 423–445. [doi:10.1007/s10237-006-0070-x](https://doi.org/10.1007/s10237-006-0070-x).
- [23] P. Ciarletta, M. Destade, A. L. Gower, On residual stresses and homeostasis: an elastic theory of functional adaptation in living matter, *Scientific Reports* 6 (1). [doi:10.1038/srep24390](https://doi.org/10.1038/srep24390).
- [24] E. Kuhl, Growing matter: A review of growth in living systems, *J. Mech. Behav. Biomed. Mater.* 29 (2014) 529–543. [doi:10.1016/j.jmbbm.2013.10.009](https://doi.org/10.1016/j.jmbbm.2013.10.009).
- [25] J. D. Humphrey, K. R. Rajagopal, A constrained mixture model for growth and remodeling of soft tissues, *Mathematical Models and Methods in Applied Sciences* 12 (03) (2002) 407–430. [doi:10.1142/s0218202502001714](https://doi.org/10.1142/s0218202502001714).
- [26] E. Rodriguez, A. Hoger, A. McCulloch, Stress-dependent finite growth in soft elastic tissues, *J. Biomech.* 27 (1994) 455–467. [doi:https://doi.org/10.1016/0021-9290\(94\)90021-3](https://doi.org/10.1016/0021-9290(94)90021-3).
- [27] L. A. Taber, Biomechanics of growth, remodeling, and morphogenesis, *Applied Mechanics Reviews* 48 (8) (1995) 487. [doi:10.1115/1.3005109](https://doi.org/10.1115/1.3005109).
- [28] M. Epstein, G. A. Maugin, Thermomechanics of volumetric growth in uniform bodies, *International Journal of Plasticity* 16 (7-8) (2000) 951–978. [doi:10.1016/s0749-6419\(99\)00081-9](https://doi.org/10.1016/s0749-6419(99)00081-9).
- [29] K. Garikipati, E. Arruda, K. Grosh, H. Narayanan, S. Calve, A continuum treatment of growth in biological tissue: the coupling of mass

- 956 transport and mechanics, *J. Mech. Phys. Solids* 52 (2004) 1595–1625.
 957 [doi:10.1016/j.jmps.2004.01.004](https://doi.org/10.1016/j.jmps.2004.01.004).
- 958 [30] B. Loret, F.M.F. Simões, A framework for deformation, generalized
 959 diffusion, mass transfer and growth in multi-species multi-phase bio-
 960 logical tissues, *Eur. J. Mech. A* 24 (2005) 757–781. [doi:10.1016/j.](https://doi.org/10.1016/j.euromechsol.2005.05.005)
 961 [euromechsol.2005.05.005](https://doi.org/10.1016/j.euromechsol.2005.05.005).
- 962 [31] R. K. Jain, J. D. Martin, T. Stylianopoulos, The role of mechanical
 963 forces in tumor growth and therapy, *Annu. Rev. Biomed. Eng.* 16 (2014)
 964 321–346. [doi:10.1146/annurev-bioeng-071813-105259](https://doi.org/10.1146/annurev-bioeng-071813-105259).
- 965 [32] M. Böl, A. B. Albero, On a new model for inhomogeneous volume growth
 966 of elastic bodies, *J. Mech. Beh. Biom. Mat.* 29 (2014) 582–593. [doi:](https://doi.org/10.1016/j.jmbbm.2013.01.027)
 967 [10.1016/j.jmbbm.2013.01.027](https://doi.org/10.1016/j.jmbbm.2013.01.027).
- 968 [33] A. Ramírez-Torres, R. Rodríguez-Ramos, J. Merodio, J. Bravo-
 969 Castillero, R. Guinovart-Díaz, J. Alfonso, Mathematical modeling of
 970 anisotropic avascular tumor growth, *Mechanics Research Communica-*
 971 *tions* 69 (2015) 8–14. [doi:10.1016/j.mechrescom.2015.06.002](https://doi.org/10.1016/j.mechrescom.2015.06.002).
- 972 [34] A. Grillo, R. Prohl, G. Wittum, A poroplastic model of structural reor-
 973 ganisation in porous media of biomechanical interest, *Continuum Mech.*
 974 *Therm.* 28 (2016) 579–601. [doi:10.1007/s00161-015-0465-y](https://doi.org/10.1007/s00161-015-0465-y).
- 975 [35] A. Grillo, R. Prohl, G. Wittum, A generalised algorithm for anelastic
 976 processes in elastoplasticity and biomechanics, *Math. Mech. Solids* 22(3)
 977 (2017) 502–527. [doi:10.1177/1081286515598661](https://doi.org/10.1177/1081286515598661).
- 978 [36] M. Mićunović, *Thermomechanics of Viscoplasticity*, Springer New York,
 979 2009. [doi:10.1007/978-0-387-89490-4](https://doi.org/10.1007/978-0-387-89490-4).
- 980 [37] S. Sadik, A. Yavari, On the origins of the idea of the multiplicative
 981 decomposition of the deformation gradient, *Mathematics and Mechanics*
 982 *of Solids* 22 (4) (2017) 771–772. [doi:10.1177/1081286515612280](https://doi.org/10.1177/1081286515612280).
- 983 [38] E. Kröner, Allgemeine Kontinuumstheorie der Versetzungen und
 984 Eigenspannungen, *Archive for Rational Mechanics and Analysis* 4 (1)
 985 (1959) 273–334. [doi:10.1007/bf00281393](https://doi.org/10.1007/bf00281393).
- 986 [39] A. Klarbring, T. Olsson, J. Stålhand, Theory of residual stresses with
 987 application to an arterial geometry, *Arch. Mech.* 59(4–5) (2007) 341–364.
- 988 [40] A. Yavari, A geometric theory of growth mechanics, *J. Nonlinear Sci.* 20
 989 (2010) 781–830. [doi:10.1007/s00332-010-9073-y](https://doi.org/10.1007/s00332-010-9073-y).

- [41] A. Yavari, A. Goriely, Weyl geometry and the nonlinear mechanics of distributed point defects, *Proc. R. Soc. A* 468 (2012) 3902–3922. doi:10.1098/rspa.2012.0342.
- [42] M. Epstein, Self-driven continuous dislocations and growth, in: M. G. Steinmann P. (Ed.), *Mechanics of Material Forces. Advances in Mechanics and Mathematics*, Vol. 11, Springer, Boston, MA, 2005, pp. 129–139. doi:10.1007/0-387-26261-x_13.
- [43] P. Ciarletta, D. Ambrosi, G. Maugin, Mass transport in morphogenetic processes: A second gradient theory for volumetric growth and material remodeling, *J. Mech. Phys. Solids* 60 (2012) 432–450. doi:10.1016/j.jmps.2011.11.011.
- [44] M. Minozzi, P. Nardinocchi, L. Teresi, V. Varano, Growth-induced compatible strains, *Math. Mech. Solids* 22 (1) (2016) 62–71. doi:10.1177/1081286515570510.
- [45] A. Goriely, *The Mathematics and Mechanics of Biological Growth*, Springer New York, 2016. doi:10.1007/978-0-387-87710-5.
- [46] P. Nardinocchi, L. Teresi, V. Varano, The elastic metric: A review of elasticity with large distortions, *Int. J. Nonlinear Mech.* 56 (2013) 34–42. doi:10.1016/j.ijnonlinmec.2013.05.002.
- [47] J. Lubliner, *Plasticity Theory*, Dover Publications, Inc., Mineola, New York, 2008.
- [48] M. Epstein, M. Elżanowski, *Material Inhomogeneities and their Evolution — A Geometric Approach*, 1st Edition, Springer-Verlag Berlin Heidelberg, 2007. doi:10.1007/978-3-540-72373-8.
- [49] M. Epstein, *The geometric language of continuum mechanics*, Cambridge University Press, 2010.
- [50] A. Menzel, Modelling of anisotropic growth in biological tissues — a new approach and computational aspects, *Biomechan. Model. Mechanobiol.* 3 (2005) 147–171. doi:10.1007/s10237-004-0047-6.
- [51] T. Olsson, A. Klarbring, Residual stresses in soft tissue as a consequence of growth and remodeling: application to an arterial geometry, *Eur. J. Mech. A* 27(6) (2008) 959–974. doi:10.1016/j.euromechsol.2007.12.006.

- [52] C. Voutouri, F. Mpekris, P. Papageorgis, A. D. Odysseos, T. Stylianopoulos, Role of constitutive behavior and tumor-host mechanical interactions in the state of stress and growth of solid tumors, PLoS ONE 9 (8) (2014) e104717. [doi:10.1371/journal.pone.0104717](https://doi.org/10.1371/journal.pone.0104717).
- [53] F. Mpekris, S. Angeli, A. P. Pirentis, T. Stylianopoulos, Stress-mediated progression of solid tumors: effect of mechanical stress on tissue oxygenation, cancer cell proliferation, and drug delivery, Biomech. Model. Mechanobiol. 14 (6) (2015) 1391–1402. [doi:10.1007/s10237-015-0682-0](https://doi.org/10.1007/s10237-015-0682-0).
- [54] P. Mascheroni, M. Carfagna, A. Grillo, D. Boso, B. Schrefler, An avascular tumor growth model based on porous media mechanics and evolving natural states, Mathematics and Mechanics of Solids 23 (4) (2018) 686–712. [doi:10.1177/1081286517711217](https://doi.org/10.1177/1081286517711217).
- [55] D. Ambrosi, L. Preziosi, On the closure of mass balance models for tumor growth, Mathematical Models and Methods in Applied Sciences 12 (05) (2002) 737–754. [doi:10.1142/s0218202502001878](https://doi.org/10.1142/s0218202502001878).
- [56] D. Ambrosi, F. Mollica, The role of stress in the growth of a multicell spheroid, J. Math. Biol. 49 (2004) 477–499. [doi:10.1007/s00285-003-0238-2](https://doi.org/10.1007/s00285-003-0238-2).
- [57] C. Giverso, M. Scianna, A. Grillo, Growing avascular tumours as elastoplastic bodies by the theory of evolving natural configurations, Mech. Res. Commun. 68 (2015) 31–39. [doi:http://dx.doi.org/10.1016/j.mechrescom.2015.04.004](https://doi.org/http://dx.doi.org/10.1016/j.mechrescom.2015.04.004).
- [58] G. Helmlinger, P. A. Netti, H. C. Lichtenbeld, R. J. Melder, R. K. Jain, Solid stress inhibits the growth of multicellular tumor spheroids, Nature Biotechnology 15 (8) (1997) 778–783. [doi:10.1038/nbt0897-778](https://doi.org/10.1038/nbt0897-778).
- [59] S. Preston, M. Elzanowski, Material uniformity and the concept of the stress space, in: B. Albers (Ed.), Continuous Media with Microstructure, 1st Edition, Springer-Verlag Berlin Heidelberg, 2010, pp. 91–101. [doi:10.1007/978-3-642-11445-8](https://doi.org/10.1007/978-3-642-11445-8).
- [60] V. Ciancio, M. Dolfi, M. Francaviglia, S. Preston, Uniform materials and the multiplicative decomposition of the deformation gradient in finite elasto-plasticity, J. Non-Equilib. Thermodyn. 33(3) (2008) 199–234. [doi:10.1515/JNETDY.2008.009](https://doi.org/10.1515/JNETDY.2008.009).

- 1058 [61] J. Marsden, T. Hughes, Mathematical Foundations of Elasticity, Dover
1059 Publications, Inc., Mineola, New York, 1983.
- 1060 [62] L. S. Bennethum, M. A. Murad, J. H. Cushman, Macroscale ther-
1061 modynamics and the chemical potential for swelling porous media,
1062 Transport in Porous Media 39 (2) (2000) 187–225. [doi:10.1023/a:
1063 1006661330427](https://doi.org/10.1023/a:1006661330427).
- 1064 [63] G. Sciarra, G. A. Maugin, K. Hutter, A variational approach to a micro-
1065 structured theory of solid-fluid mixtures, Archive of Applied Mechanics
1066 73 (2003) 194–224. [doi:10.1007/s00419-003-0279-4](https://doi.org/10.1007/s00419-003-0279-4).
- 1067 [64] R. Serpieri, F. Travascio, Variational continuum multiphase poroelastic-
1068 ity, Springer Singapore, 2017. [doi:10.1007/978-981-10-3452-7](https://doi.org/10.1007/978-981-10-3452-7).
- 1069 [65] G. Ateshian, J. Weiss, Anisotropic hydraulic permeability under finite
1070 deformation, J. Biomech. Engng. 132 (2010) 111004–1–111004–7. [doi:
1071 10.1115/1.4002588](https://doi.org/10.1115/1.4002588).
- 1072 [66] M. H. Holmes, V. C. Mow, The nonlinear characteristics of soft gels and
1073 hydrated connective tissues in ultrafiltration., Journal of biomechanics
1074 23 (1990) 1145–1156. [doi:10.1016/0021-9290\(90\)90007-P](https://doi.org/10.1016/0021-9290(90)90007-P).
- 1075 [67] S. Cleja-Tigoiu, G. A. Maugin, Eshelby’s stress tensors in finite elasto-
1076 plasticity, Acta Mechanica 139 (1-4) (2000) 231–249. [doi:10.1007/
1077 bf01170191](https://doi.org/10.1007/bf01170191).
- 1078 [68] A. Tomic, A. Grillo, S. Federico, Poroelastic materials reinforced by
1079 statistically oriented fibres — numerical implementation and application
1080 to articular cartilage, IMA J. Appl. Math. 79 (2014) 1027–1059. [doi:
1081 10.1093/imamat/hxu039](https://doi.org/10.1093/imamat/hxu039).
- 1082 [69] A. Bazykin, Nonlinear dynamics of interacting populations, World Sci-
1083 entific Publishing, Singapore New Jersey London Hong Kong, 1998.
- 1084 [70] T. Stylianopoulos, J. D. Martin, M. Snuderl, F. Mpekris, S. R. Jain,
1085 R. K. Jain, Coevolution of solid stress and interstitial fluid pressure
1086 in tumors during progression: Implications for vascular collapse, Can-
1087 cer Research 73 (13) (2013) 3833–3841. [doi:10.1158/0008-5472.
1088 can-12-4521](https://doi.org/10.1158/0008-5472.can-12-4521).
- 1089 [71] M. A. J. Chaplain, L. Graziano, L. Preziosi, Mathematical modelling
1090 of the loss of tissue compression responsiveness and its role in solid
1091 tumour development, Mathematical Medicine and Biology: A Journal
1092 of the IMA 23 (3) (2006) 197–229. [doi:10.1093/imammb/dql009](https://doi.org/10.1093/imammb/dql009).

- 1093 [72] J. J. Casciari, S. V. Sotirchos, R. M. Sutherland, Mathematical mod-
 1094 elling of microenvironment and growth in EMT6/ro multicellular tu-
 1095 mour spheroids, *Cell Proliferation* 25 (1) (1992) 1–22. [doi:10.1111/j.](https://doi.org/10.1111/j.1365-2184.1992.tb01433.x)
 1096 [1365-2184.1992.tb01433.x](https://doi.org/10.1111/j.1365-2184.1992.tb01433.x).
- 1097 [73] J. J. Casciari, S. V. Sotirchos, R. M. Sutherland, Variations in tumor cell
 1098 growth rates and metabolism with oxygen concentration, glucose con-
 1099 centration, and extracellular pH, *Journal of Cellular Physiology* 151 (2)
 1100 (1992) 386–394. [doi:10.1002/jcp.1041510220](https://doi.org/10.1002/jcp.1041510220).
- 1101 [74] P. Mascheroni, C. Stigliano, M. Carfagna, D. P. Boso, L. Preziosi,
 1102 P. Decuzzi, B. A. Schrefler, Predicting the growth of glioblas-
 1103 toma multiforme spheroids using a multiphase porous media model,
 1104 *Biomech. Model. Mechanobiol.* 15 (5) (2016) 1215–1228. [doi:10.1007/](https://doi.org/10.1007/s10237-015-0755-0)
 1105 [s10237-015-0755-0](https://doi.org/10.1007/s10237-015-0755-0).